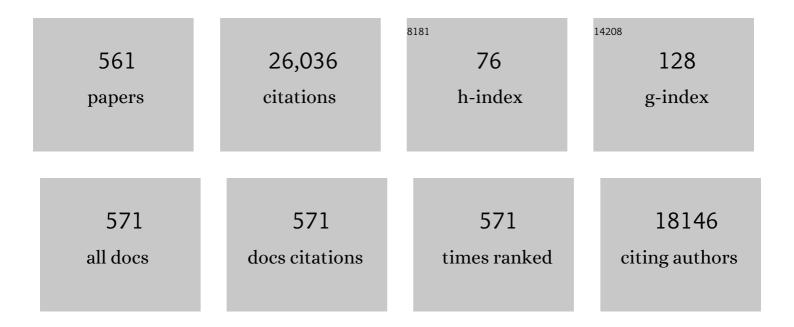
Jeong Min Lee

List of Publications by Year in descending order

Source: https://exaly.com/author-pdf/7449861/publications.pdf Version: 2024-02-01



#	Article	IF	CITATIONS
1	Simultaneous evaluation of perfusion and morphology using GRASP MRI in hepatic fibrosis. European Radiology, 2022, 32, 34-45.	4.5	8
2	LI-RADS v2018: how to appropriately use ancillary features in category adjustment from intermediate probability of malignancy (LR-3) to probably HCC (LR-4) on gadoxetic acid–enhanced MRI. European Radiology, 2022, 32, 46-55.	4.5	5
3	How to approach pancreatic cancer after neoadjuvant treatment: assessment of resectability using multidetector CT and tumor markers. European Radiology, 2022, 32, 56-66.	4.5	11
4	LI-RADS Tumor in Vein at CT and Hepatobiliary MRI. Radiology, 2022, 302, 107-115.	7.3	13
5	Risk Factors for Hypervascularization in Hepatobiliary Phase Hypointense Nodules without Arterial Phase Hyperenhancement: A Systematic Review and Meta-analysis. Academic Radiology, 2022, 29, 198-210.	2.5	5
6	Assessment of the inter-platform reproducibility of ultrasound attenuation examination in nonalcoholic fatty liver disease. Ultrasonography, 2022, 41, 355-364.	2.3	11
7	Image quality in liver CT: low-dose deep learning vs standard-dose model-based iterative reconstructions. European Radiology, 2022, 32, 2865-2874.	4.5	26
8	CT/MRI and CEUS LI-RADS Major Features Association with Hepatocellular Carcinoma: Individual Patient Data Meta-Analysis. Radiology, 2022, 302, 326-335.	7.3	32
9	Diagnostic Performance of Spin-Echo Echo-Planar Imaging Magnetic Resonance Elastography in 3T System for Noninvasive Assessment of Hepatic Fibrosis. Korean Journal of Radiology, 2022, 23, 180.	3.4	4
10	Quantitative Evaluation of Hepatic Steatosis Using Advanced Imaging Techniques: Focusing on New Quantitative Ultrasound Techniques. Korean Journal of Radiology, 2022, 23, 13.	3.4	18
11	Subtype Classification of Intrahepatic Cholangiocarcinoma Using Liver MR Imaging Features and Its Prognostic Value. Liver Cancer, 2022, 11, 233-246.	7.7	8
12	Dual-Energy CT for Risk of Postoperative Pancreatic Fistula. Radiology, 2022, , 220320.	7.3	1
13	Impact of Reference Standard on CT, MRI, and Contrast-enhanced US LI-RADS Diagnosis of Hepatocellular Carcinoma: A Meta-Analysis. Radiology, 2022, 303, 544-545.	7.3	15
14	Accelerated Pancreatobiliary <scp>MRI</scp> for Pancreatic Cancer Surveillance in Patients With Pancreatic Cystic Neoplasms. Journal of Magnetic Resonance Imaging, 2022, 56, 1757-1768.	3.4	2
15	Deep learning–based image reconstruction of 40-keV virtual monoenergetic images of dual-energy CT for the assessment of hypoenhancing hepatic metastasis. European Radiology, 2022, 32, 6407-6417.	4.5	11
16	Imaging diagnosis of hepatocellular carcinoma: Future directions with special emphasis on hepatobiliary magnetic resonance imaging and contrast-enhanced ultrasound. Clinical and Molecular Hepatology, 2022, 28, 362-379.	8.9	17
17	Multidetector CT of Extrahepatic Bile Duct Cancer: Diagnostic Performance of Tumor Resectability and Interreader Agreement. Radiology, 2022, 304, 96-105.	7.3	4
18	Comparison of a preoperative MR-based recurrence risk score versus the postoperative score and four clinical staging systems in hepatocellular carcinoma: a retrospective cohort study. European Radiology, 2022, 32, 7578-7589.	4.5	5

#	Article	IF	CITATIONS
19	Identifying high-risk colon cancer on CT an a radiomics signature improve radiologist's performance for T staging?. Abdominal Radiology, 2022, 47, 2739-2746.	2.1	4
20	Perfluorobutane-enhanced ultrasonography with a Kupffer phase: improved diagnostic sensitivity for hepatocellular carcinoma. European Radiology, 2022, 32, 8507-8517.	4.5	8
21	Deep learning-based reconstruction of virtual monoenergetic images of kVp-switching dual energy CT for evaluation of hypervascular liver lesions: Comparison with standard reconstruction technique. European Journal of Radiology, 2022, 154, 110390.	2.6	7
22	Detection of distant metastases in rectal cancer: contrast-enhanced CT vs whole body MRI. European Radiology, 2021, 31, 104-111.	4.5	2
23	Evaluation of Primary Liver Cancers Using Hepatocyteâ€Specific Contrastâ€Enhanced <scp>MRI</scp> : Pitfalls and Potential Tips. Journal of Magnetic Resonance Imaging, 2021, 53, 655-675.	3.4	3
24	Clinical Feasibility of Quantitative Ultrasound Imaging for Suspected Hepatic Steatosis: Intra- and Inter-examiner Reliability and Correlation with Controlled Attenuation Parameter. Ultrasound in Medicine and Biology, 2021, 47, 438-445.	1.5	19
25	Tumor Stiffness Measurements on MR Elastography for Single Nodular Hepatocellular Carcinomas Can Predict Tumor Recurrence After Hepatic Resection. Journal of Magnetic Resonance Imaging, 2021, 53, 587-596.	3.4	21
26	Clinical outcomes of patients with a high alpha-fetoprotein level but without evident recurrence on CT or MRI in surveillance after curative-intent treatment for hepatocellular carcinoma. Abdominal Radiology, 2021, 46, 597-606.	2.1	3
27	Intra-individual comparison of dual portal venous phases for non-invasive diagnosis of hepatocellular carcinoma at gadoxetic acid–enhanced liver MRI. European Radiology, 2021, 31, 824-833.	4.5	5
28	Impact of respiratory motion on liver stiffness measurements according to different shear wave elastography techniques and region of interest methods: a phantom study. Ultrasonography, 2021, 40, 103-114.	2.3	8
29	Additional Value of Integrated ¹⁸ F-FDG PET/MRI for Evaluating Biliary Tract Cancer: Comparison with Contrast-Enhanced CT. Korean Journal of Radiology, 2021, 22, 714.	3.4	5
30	Role of Contrast-Enhanced Ultrasound as a Second-Line Diagnostic Modality in Noninvasive Diagnostic Algorithms for Hepatocellular Carcinoma. Korean Journal of Radiology, 2021, 22, 354.	3.4	21
31	Radiofrequency Ablation Using a Separable Clustered Electrode for the Treatment of Hepatocellular Carcinomas: A Randomized Controlled Trial of a Dual-Switching Monopolar Mode Versus a Single-Switching Monopolar Mode. Korean Journal of Radiology, 2021, 22, 179.	3.4	8
32	Quantitative Ultrasound Radiofrequency Data Analysis for the Assessment of Hepatic Steatosis in Nonalcoholic Fatty Liver Disease Using Magnetic Resonance Imaging Proton Density Fat Fraction as the Reference Standard. Korean Journal of Radiology, 2021, 22, 1077.	3.4	32
33	Volumetric CT Texture Analysis of Intrahepatic Mass-Forming Cholangiocarcinoma for the Prediction of Postoperative Outcomes: Fully Automatic Tumor Segmentation Versus Semi-Automatic Segmentation. Korean Journal of Radiology, 2021, 22, 1797-1808.	3.4	3
34	Consensus report from the 9th International Forum for Liver Magnetic Resonance Imaging: applications of gadoxetic acid-enhanced imaging. European Radiology, 2021, 31, 5615-5628.	4.5	14
35	Comparison of low kVp CT and dual-energy CT for the evaluation of hypervascular hepatocellular carcinoma. Abdominal Radiology, 2021, 46, 3217-3226.	2.1	10
36	Hepatic fibrosis grading with extracellular volume fraction from iodine mapping in spectral liver CT. European Journal of Radiology, 2021, 137, 109604.	2.6	17

#	Article	IF	CITATIONS
37	CT for lymph node staging of Colon cancer: not only size but also location and number of lymph node count. Abdominal Radiology, 2021, 46, 4096-4105.	2.1	23
38	Ultrasound-guided transient elastography and two-dimensional shear wave elastography for assessment of liver fibrosis: emphasis on technical success and reliable measurements. Ultrasonography, 2021, 40, 217-227.	2.3	8
39	Comparisons between image quality and diagnostic performance of 2D- and breath-hold 3D magnetic resonance cholangiopancreatography at 3T. European Radiology, 2021, 31, 8399-8407.	4.5	6
40	Radio-pathologic correlation of biphenotypic primary liver cancer (combined hepatocellular) Tj ETQq0 0 0 rgBT /C liver MRI. European Radiology, 2021, 31, 9479-9488.	Overlock 10 4.5	0 Tf 50 627 To 8
41	Evaluation of LI-RADS Version 2018 Treatment Response Algorithm for Hepatocellular Carcinoma in Liver Transplant Candidates: Intraindividual Comparison between CT and Hepatobiliary Agent–enhanced MRI. Radiology, 2021, 299, 336-345.	7.3	13
42	Early response evaluation of doxorubicin-nanoparticle-microbubble therapy in orthotopic hepatocellular carcinoma rat model using contrast-enhanced ultrasound and intravoxel incoherent motion-diffusion MRI. Ultrasonography, 2021, , .	2.3	2
43	Comparison of the Effects of Hepatic Steatosis on Monoexponential DWI, Intravoxel Incoherent Motion Diffusion-weighted Imaging and Diffusion Kurtosis Imaging. Academic Radiology, 2021, 28, S203-S209.	2.5	4
44	Systematic review and meta-analysis of diagnostic performance of CT imaging for assessing resectability of pancreatic ductal adenocarcinoma after neoadjuvant therapy: importance of CT criteria. Abdominal Radiology, 2021, 46, 5201-5217.	2.1	10
45	Utility of Real-time CT/MRI-US Automatic Fusion System Based on Vascular Matching in Percutaneous Radiofrequency Ablation for Hepatocellular Carcinomas: A Prospective Study. CardioVascular and Interventional Radiology, 2021, 44, 1579-1596.	2.0	6
46	Outcome of No-Touch Radiofrequency Ablation for Small Hepatocellular Carcinoma: A Multicenter Clinical Trial. Radiology, 2021, 301, 229-236.	7.3	41
47	Diagnostic Performance of 2018 KLCA-NCC Practice Guideline for Hepatocellular Carcinoma on Gadoxetic Acid-Enhanced MRI in Patients with Chronic Hepatitis B or Cirrhosis: Comparison with LI-RADS Version 2018. Korean Journal of Radiology, 2021, 22, 1066.	3.4	12
48	Laparoscopic Liver Resection versus Percutaneous Radiofrequency Ablation for Small Single Nodular Hepatocellular Carcinoma: Comparison of Treatment Outcomes. Liver Cancer, 2021, 10, 25-37.	7.7	38
49	Quantitative ultrasound radiofrequency data analysis for the assessment of hepatic steatosis using the controlled attenuation parameter as a reference standard. Ultrasonography, 2021, 40, 136-146.	2.3	25
50	Radiologic Evaluation and Structured Reporting Form for Extrahepatic Bile Duct Cancer: 2019 Consensus Recommendations from the Korean Society of Abdominal Radiology. Korean Journal of Radiology, 2021, 22, 41.	3.4	19
51	Switching Monopolar No-Touch Radiofrequency Ablation Using Octopus Electrodes for Small Hepatocellular Carcinoma: A Randomized Clinical Trial. Liver Cancer, 2021, 10, 72-81.	7.7	19
52	No-Touch vs. Conventional Radiofrequency Ablation Using Twin Internally Cooled Wet Electrodes for Small Hepatocellular Carcinomas: A Randomized Prospective Comparative Study. Korean Journal of Radiology, 2021, 22, 1974.	3.4	18
53	Reduced field-of-view versus full field-of-view diffusion-weighted imaging for the evaluation of complete response to neoadjuvant chemoradiotherapy in patients with locally advanced rectal cancer. Abdominal Radiology, 2021, 46, 1468-1477.	2.1	13
54	Comparison of Overall Survival between Surgical Resection and Radiofrequency Ablation for Hepatitis B-Related Hepatocellular Carcinoma. Cancers, 2021, 13, 6009.	3.7	9

#	Article	IF	CITATIONS
55	Two-dimensional Shear Wave Elastography with Propagation Maps for the Assessment of Liver Fibrosis and Clinically Significant Portal Hypertension in Patients with Chronic Liver Disease: A Prospective Study. Academic Radiology, 2020, 27, 798-806.	2.5	12
56	Consensus report from the 8th International Forum for Liver Magnetic Resonance Imaging. European Radiology, 2020, 30, 370-382.	4.5	55
57	CT and MR imaging findings of the livers in adults with Fontan palliation: an observational study. Abdominal Radiology, 2020, 45, 188-202.	2.1	15
58	Initial M Staging of Rectal Cancer: FDG PET/MRI with a Hepatocyte-specific Contrast Agent versus Contrast-enhanced CT. Radiology, 2020, 294, 310-319.	7.3	31
59	Hepatobiliary phase hypointense nodule without arterial phase hyperenhancement: are they at risk of HCC recurrence after ablation or surgery? A systematic review and meta-analysis. European Radiology, 2020, 30, 1624-1633.	4.5	12
60	How to Best Detect Portal Vein Tumor Thrombosis in Patients with Hepatocellular Carcinoma Meeting the Milan Criteria: Gadoxetic Acid-Enhanced MRI versus Contrast-Enhanced CT. Liver Cancer, 2020, 9, 293-307.	7.7	24
61	Contrast-enhanced US with Sulfur Hexafluoride and Perfluorobutane for the Diagnosis of Hepatocellular Carcinoma in Individuals with High Risk. Radiology, 2020, 297, 108-116.	7.3	32
62	Diagnostic Performance of LI-RADS Treatment Response Algorithm for Hepatocellular Carcinoma: Adding Ancillary Features to MRI Compared with Enhancement Patterns at CT and MRI. Radiology, 2020, 296, 554-561.	7.3	35
63	Diagnostic Value of High Frame Rate Contrast-enhanced Ultrasonography and Post-processing Contrast Vector Imaging for Evaluation of Focal Liver Lesions: A Feasibility Study. Ultrasound in Medicine and Biology, 2020, 46, 2254-2264.	1.5	3
64	latrogenic Arterioportal Fistula Caused by Radiofrequency Ablation of Hepatocellular Carcinoma: Clinical Course and Treatment Outcomes. Journal of Vascular and Interventional Radiology, 2020, 31, 728-736.	0.5	4
65	A Comparison of Biannual Two-Phase Low-Dose Liver CT and US for HCC Surveillance in a Group at High Risk of HCC Development. Liver Cancer, 2020, 9, 503-517.	7.7	40
66	Prediction of microvascular invasion of hepatocellular carcinoma: value of volumetric iodine quantification using preoperative dual-energy computed tomography. Cancer Imaging, 2020, 20, 60.	2.8	13
67	Clinical Feasibility of Abbreviated Magnetic Resonance With Breath-Hold 3-Dimensional Magnetic Resonance Cholangiopancreatography for Surveillance of Pancreatic Intraductal Papillary Mucinous Neoplasm. Investigative Radiology, 2020, 55, 262-269.	6.2	15
68	Radiologic-Pathologic Correlation of Hepatobiliary Phase Hypointense Nodules without Arterial Phase Hyperenhancement at Gadoxetic Acid–enhanced MRI: A Multicenter Study. Radiology, 2020, 296, 335-345.	7.3	42
69	LI-RADS M (LR-M) criteria and reporting algorithm of v2018: diagnostic values in the assessment of primary liver cancers on gadoxetic acid-enhanced MRI. Abdominal Radiology, 2020, 45, 2440-2448.	2.1	21
70	Cardiovascular and abdominal flow alterations in adults with morphologic evidence of liver disease post Fontan palliation. International Journal of Cardiology, 2020, 317, 63-69.	1.7	3
71	Double Low-Dose Dual-Energy Liver CT in Patients at High-Risk of HCC. Investigative Radiology, 2020, 55, 340-348.	6.2	28
72	Assessing Liver Function in Liver Tumors Patients: The Performance of T1 Mapping and Residual Liver Volume on Gd-EOBDTPA-Enhanced MRI. Frontiers in Medicine, 2020, 7, 215.	2.6	5

#	Article	IF	CITATIONS
73	LI-RADS treatment response categorization on gadoxetic acid-enhanced MRI: diagnostic performance compared to mRECIST and added value of ancillary features. European Radiology, 2020, 30, 2861-2870.	4.5	37
74	Comparison of guidelines for diagnosis of hepatocellular carcinoma using gadoxetic acid–enhanced MRI in transplantation candidates. European Radiology, 2020, 30, 4762-4771.	4.5	20
75	Radiofrequency ablation using internally cooled wet electrodes in bipolar mode for the treatment of recurrent hepatocellular carcinoma after locoregional treatment: A randomized prospective comparative study. PLoS ONE, 2020, 15, e0239733.	2.5	8
76	Assessment of liver fibrosis using 2-dimensional shear wave elastography: a prospective study of intra- and inter-observer repeatability and comparison with point shear wave elastography. Ultrasonography, 2020, 39, 52-59.	2.3	21
77	Comparison of MicroFlow Imaging with color and power Doppler imaging for detecting and characterizing blood flow signals in hepatocellular carcinoma. Ultrasonography, 2020, 39, 85-93.	2.3	29
78	Reproducibility of ultrasound attenuation imaging for the noninvasive evaluation of hepatic steatosis. Ultrasonography, 2020, 39, 121-129.	2.3	51
79	Combined Hepatocellular-Cholangiocarcinoma: Changes in the 2019 World Health Organization Histological Classification System and Potential Impact on Imaging-Based Diagnosis. Korean Journal of Radiology, 2020, 21, 1115.	3.4	24
80	Clinicoradiological features of resected serous cystic neoplasms according to morphological subtype and preoperative tentative diagnosis: can radiological characteristics distinguish serous cystic neoplasms from other lesions?. Annals of Surgical Treatment and Research, 2020, 98, 247.	1.0	5
81	Second-look breast ultrasonography after galactography in patients with nipple discharge. Medical Ultrasonography, 2020, 1, 58.	0.8	4
82	Combined hepatocellular cholangiocarcinoma: LI-RADS v2017 categorisation for differential diagnosis and prognostication on gadoxetic acid-enhanced MR imaging. European Radiology, 2019, 29, 373-382.	4.5	89
83	Added Value of sequentially performed gadoxetic acidâ€enhanced liver MRI for the diagnosis of small (10–19 mm) or atypical hepatic observations at contrastâ€enhanced CT: A prospective comparison. Journal of Magnetic Resonance Imaging, 2019, 49, 574-587.	3.4	18
84	Hepatic nontuberculous mycobacterial granulomas in patients with cancer mimicking metastases: an analysis of three cases. Quantitative Imaging in Medicine and Surgery, 2019, 9, 1126-1131.	2.0	4
85	Atypical Appearance of Hepatocellular Carcinoma and Its Mimickers: How to Solve Challenging Cases Using Gadoxetic Acid-Enhanced Liver Magnetic Resonance Imaging. Korean Journal of Radiology, 2019, 20, 1019.	3.4	36
86	Prospective Validation of Repeatability of Shear Wave Dispersion Imaging for Evaluation of Non-alcoholic Fatty Liver Disease. Ultrasound in Medicine and Biology, 2019, 45, 2688-2696.	1.5	13
87	LI-RADS Version 2017 versus Version 2018: Diagnosis of Hepatocellular Carcinoma on Gadoxetate Disodium–enhanced MRI. Radiology, 2019, 292, 655-663.	7.3	55
88	FRI-485-Laparoscopic liver resection vs. Percutaneous radiofrequency ablation for small single nodular HCC: Comparison of treatment outcome. Journal of Hepatology, 2019, 70, e611-e613.	3.7	1
89	Preoperative CT Classification of the Resectability of Pancreatic Cancer: Interobserver Agreement. Radiology, 2019, 293, 343-349.	7.3	46
90	Value of virtual monochromatic spectral image of dual-layer spectral detector CT with noise reduction algorithm for image quality improvement in obese simulated body phantom. BMC Medical Imaging, 2019, 19, 76.	2.7	14

#	Article	IF	CITATIONS
91	Emerging Role of Hepatobiliary Magnetic Resonance Contrast Media and Contrast-Enhanced Ultrasound for Noninvasive Diagnosis of Hepatocellular Carcinoma: Emphasis on Recent Updates in Major Guidelines. Korean Journal of Radiology, 2019, 20, 863.	3.4	23
92	Hepatocellular Carcinoma: Texture Analysis of Preoperative Computed Tomography Images Can Provide Markers of Tumor Grade and Disease-Free Survival. Korean Journal of Radiology, 2019, 20, 569.	3.4	43
93	High Acceleration Three-Dimensional T1-Weighted Dual Echo Dixon Hepatobiliary Phase Imaging Using Compressed Sensing-Sensitivity Encoding: Comparison of Image Quality and Solid Lesion Detectability with the Standard T1-Weighted Sequence. Korean Journal of Radiology, 2019, 20, 438.	3.4	32
94	Evaluation of the Impact of Iterative Reconstruction Algorithms on Computed Tomography Texture Features of the Liver Parenchyma Using the Filtration-Histogram Method. Korean Journal of Radiology, 2019, 20, 558.	3.4	14
95	Comparison of monoexponential, intravoxel incoherent motion diffusion-weighted imaging and diffusion kurtosis imaging for assessment of hepatic fibrosis. Acta Radiologica, 2019, 60, 1593-1601.	1.1	11
96	Prospective Evaluation of Hepatic Steatosis Using Ultrasound Attenuation Imaging in Patients with Chronic Liver Disease with Magnetic Resonance Imaging Proton Density Fat Fraction as the Reference Standard. Ultrasound in Medicine and Biology, 2019, 45, 1407-1416.	1.5	72
97	Whole tumor ablation of locally recurred hepatocellular carcinoma including retained iodized oil after transarterial chemoembolization improves progression-free survival. European Radiology, 2019, 29, 5052-5062.	4.5	7
98	Clinical Feasibility of Gadoxetic Acid–Enhanced Isotropic High-Resolution 3-Dimensional Magnetic Resonance Cholangiography Using an Iterative Denoising Algorithm for Evaluation of the Biliary Anatomy of Living Liver Donors. Investigative Radiology, 2019, 54, 103-109.	6.2	20
99	Man or machine? Prospective comparison of the version 2018 EASL, LI-RADS criteria and a radiomics model to diagnose hepatocellular carcinoma. Cancer Imaging, 2019, 19, 84.	2.8	36
100	Can MRI Features Predict Prognosis in Mass-forming Intrahepatic Cholangiocarcinoma?. Radiology, 2019, 290, 700-701.	7.3	2
101	Non-hypervascular hepatobiliary phase hypointense nodules on gadoxetic acid-enhanced MR can help determine the treatment method for HCC. European Radiology, 2019, 29, 3122-3131.	4.5	17
102	Quantitative Assessment of Liver Function by Using Gadoxetic Acid–enhanced MRI: Hepatocyte Uptake Ratio. Radiology, 2019, 290, 125-133.	7.3	59
103	Retrospective validation of a new diagnostic criterion for hepatocellular carcinoma on gadoxetic acid-enhanced MRI: can hypointensity on the hepatobiliary phase be used as an alternative to washout with the aid of ancillary features?. European Radiology, 2019, 29, 1724-1732.	4.5	76
104	Comparison of four different Shear Wave Elastography platforms according to abdominal wall thickness in liver fibrosis evaluation: a phantom study. Medical Ultrasonography, 2019, 21, 22.	0.8	15
105	Usefulness of contrast-enhanced ultrasound using perfluorobutanecontaining microbubbles as a planning for percutaneous biopsies of focal hepatic lesions: a prospective feasibility study. Medical Ultrasonography, 2019, 21, 109.	0.8	4
106	Reproducibility of liver stiffness measurements made with two different 2-dimensional shear wave elastography systems using the comb-push technique. Ultrasonography, 2019, 38, 246-254.	2.3	14
107	Inter-platform reproducibility of liver stiffness measured with two different point shear wave elastography techniques and 2-dimensional shear wave elastography using the comb-push technique. Ultrasonography, 2019, 38, 345-354.	2.3	7
108	Contrast-enhanced ultrasound approach to the diagnosis of focal liver lesions: the importance of washout. Ultrasonography, 2019, 38, 289-301.	2.3	36

#	Article	IF	CITATIONS
109	Rapid Imaging: Recent Advances in Abdominal MRI for Reducing Acquisition Time and Its Clinical Applications. Korean Journal of Radiology, 2019, 20, 1597.	3.4	50
110	Microvascular Flow Imaging of Residual or Recurrent Hepatocellular Carcinoma after Transarterial Chemoembolization: Comparison with Color/Power Doppler Imaging. Korean Journal of Radiology, 2019, 20, 1114.	3.4	22
111	Validation of a New Point Shear-Wave Elastography Method for Noninvasive Assessment of Liver Fibrosis: A Prospective Multicenter Study. Korean Journal of Radiology, 2019, 20, 1527.	3.4	20
112	Comparison of international guidelines for noninvasive diagnosis of hepatocellular carcinoma: 2018 update. Clinical and Molecular Hepatology, 2019, 25, 245-263.	8.9	154
113	2018 Korean Liver Cancer Association–National Cancer Center Korea Practice Guidelines for the Management of Hepatocellular Carcinoma. Gut and Liver, 2019, 13, 227-299.	2.9	255
114	Oncological Benefits of Neoadjuvant Chemoradiation With Gemcitabine Versus Upfront Surgery in Patients With Borderline Resectable Pancreatic Cancer. Annals of Surgery, 2018, 268, 215-222.	4.2	497
115	Preoperative MDCT Assessment of Resectability in Borderline Resectable Pancreatic Cancer: Effect of Neoadjuvant Chemoradiation Therapy. American Journal of Roentgenology, 2018, 210, 1059-1065.	2.2	21
116	Prognostic Role of Liver Stiffness Measurements Using Magnetic Resonance Elastography in Patients with Compensated Chronic Liver Disease. European Radiology, 2018, 28, 3513-3521.	4.5	24
117	Additional value of contrast-enhanced ultrasonography for fusion-guided, percutaneous biopsies of focal liver lesions: prospective feasibility study. Abdominal Radiology, 2018, 43, 3279-3287.	2.1	13
118	Liver Stiffness Measured by Two-Dimensional Shear-Wave Elastography: Prognostic Value after Radiofrequency Ablation for Hepatocellular Carcinoma. Liver Cancer, 2018, 7, 65-75.	7.7	23
119	Abdominal imaging findings in adult patients with Fontan circulation. Insights Into Imaging, 2018, 9, 357-367.	3.4	29
120	Clinical utility of real-time ultrasound-multimodality fusion guidance for percutaneous biopsy of focal liver lesions. European Journal of Radiology, 2018, 103, 76-83.	2.6	13
121	CT diagnosis of gallbladder adenomyomatosis: importance of enhancing mucosal epithelium, the "cotton ball sign― European Radiology, 2018, 28, 3573-3582.	4.5	16
122	GRASE Revisited: breath-hold three-dimensional (3D) magnetic resonance cholangiopancreatography using a Gradient and Spin Echo (GRASE) technique at 3T. European Radiology, 2018, 28, 3721-3728.	4.5	32
123	Magnetic resonance with diffusion-weighted imaging improves assessment of focal liver lesions in patients with potentially resectable pancreatic cancer on CT. European Radiology, 2018, 28, 3484-3493.	4.5	42
124	Focal Nodular Hyperplasia After Treatment With Oxaliplatin: A Multiinstitutional Series of Cases Diagnosed at MRI. American Journal of Roentgenology, 2018, 210, 775-779.	2.2	31
125	Gastrointestinal tract complications after hepatic radiofrequency ablation: CT prediction for major complications. Abdominal Radiology, 2018, 43, 583-592.	2.1	8
126	Clinical Outcomes of Radiofrequency Ablation for Early Hypovascular HCC: A Multicenter Retrospective Study. Radiology, 2018, 286, 338-349.	7.3	27

#	Article	IF	CITATIONS
127	Evaluation of Transient Motion During Gadoxetic Acid–Enhanced Multiphasic Liver Magnetic Resonance Imaging Using Free-Breathing Golden-Angle Radial Sparse Parallel Magnetic Resonance Imaging. Investigative Radiology, 2018, 53, 52-61.	6.2	41
128	Progression of Pancreatic Branch Duct Intraductal Papillary Mucinous Neoplasm Associates With Cyst Size. Gastroenterology, 2018, 154, 576-584.	1.3	91
129	Initial Alpha-Fetoprotein Response Predicts Prognosis in Hepatitis B-related Solitary HCC Patients After Radiofrequency Ablation. Journal of Clinical Gastroenterology, 2018, 52, e18-e26.	2.2	13
130	Principles for evaluating the clinical implementation of novel digital healthcare devices. Journal of the Korean Medical Association, 2018, 61, 765.	0.3	16
131	Huge and recurrent undifferentiated carcinoma with osteoclast-like giant cells of the pancreas. Quantitative Imaging in Medicine and Surgery, 2018, 8, 457-460.	2.0	11
132	Alteration of MRP2 expression and the graft outcome after liver transplantation. Annals of Surgical Treatment and Research, 2018, 95, 249.	1.0	2
133	No-Touch Radiofrequency Ablation of VX2 Hepatic Tumors <i>In Vivo</i> in Rabbits: A Proof of Concept Study. Korean Journal of Radiology, 2018, 19, 1099.	3.4	9
134	Prediction of Local Tumor Progression after Radiofrequency Ablation (RFA) of Hepatocellular Carcinoma by Assessment of Ablative Margin Using Pre-RFA MRI and Post-RFA CT Registration. Korean Journal of Radiology, 2018, 19, 1053.	3.4	28
135	Recommendation for terminology: Nodules without arterial phase hyperenhancement and with hepatobiliary phase hypointensity in chronic liver disease. Journal of Magnetic Resonance Imaging, 2018, 48, 1169-1171.	3.4	27
136	Differential Effect of HCV Eradication and Fibrosis Grade on Hepatocellular Carcinoma and All-cause Mortality. Scientific Reports, 2018, 8, 13651.	3.3	7
137	Hepatic epithelioid hemangioendothelioma: Challenges in the preoperative diagnosis. Kaohsiung Journal of Medical Sciences, 2018, 34, 659-661.	1.9	4
138	A prospective randomized study comparing radiofrequency ablation and hepatic resection for hepatocellular carcinoma. Annals of Surgical Treatment and Research, 2018, 94, 74.	1.0	56
139	Recent Advances in the Image-Guided Tumor Ablation of Liver Malignancies: Radiofrequency Ablation with Multiple Electrodes, Real-Time Multimodality Fusion Imaging, and New Energy Sources. Korean Journal of Radiology, 2018, 19, 545.	3.4	53
140	Magnetic resonance elastography of healthy livers at 3.0 T: Normal liver stiffness measured by SE-EPI and GRE. European Journal of Radiology, 2018, 107, 46-53.	2.6	12
141	Imaging Diagnosis of Intrahepatic and Perihilar Cholangiocarcinoma: Recent Advances and Challenges. Radiology, 2018, 288, 7-13.	7.3	145
142	Comparison of switching bipolar ablation with multiple cooled wet electrodes and switching monopolar ablation with separable clustered electrode in treatment of small hepatocellular carcinoma: A randomized controlled trial. PLoS ONE, 2018, 13, e0192173.	2.5	14
143	Additional values of highâ€resolution gadoxetic acidâ€enhanced MR cholangiography for evaluating the biliary anatomy of living liver donors: Comparison with <i>T</i> ₂ â€weighted MR cholangiography and conventional gadoxetic acidâ€enhanced MR cholangiography. Journal of Magnetic Resonance Imaging, 2018, 47, 152-159.	3.4	10
144	Disease of the Gallbladder and Biliary Tree. IDKD Springer Series, 2018, , 49-56.	0.8	5

#	Article	IF	CITATIONS
145	Intrahepatic Mass-Forming Cholangiocarcinoma: Relationship Between Computed Tomography Characteristics and Histological Subtypes. Journal of Computer Assisted Tomography, 2018, 42, 340-349.	0.9	14
146	Sub-classification of Advanced-Stage Hepatocellular Carcinoma: A Cohort Study Including 612 Patients Treated with Sorafenib. Cancer Research and Treatment, 2018, 50, 366-373.	3.0	15
147	Assessment of the Surveillance Interval at 1 Year after Curative Treatment in Hepatocellular Carcinoma: Risk Stratification. Gut and Liver, 2018, 12, 571-582.	2.9	6
148	Whole-body PET/MRI for colorectal cancer staging: Is it the way forward?. Journal of Magnetic Resonance Imaging, 2017, 45, 21-35.	3.4	31
149	Nonhypervascular Pancreatic Neuroendocrine Tumors: Differential Diagnosis from Pancreatic Ductal Adenocarcinomas at MR Imaging—Retrospective Cross-sectional Study. Radiology, 2017, 284, 77-87.	7.3	77
150	Value of Nonrigid Registration of Pre-Procedure MR with Post-Procedure CT After Radiofrequency Ablation for Hepatocellular Carcinoma. CardioVascular and Interventional Radiology, 2017, 40, 873-883.	2.0	12
151	Antiplatelet therapy and the risk of hepatocellular carcinoma in chronic hepatitis B patients on antiviral treatment. Hepatology, 2017, 66, 1556-1569.	7.3	92
152	Asia–Pacific clinical practice guidelines on the management of hepatocellular carcinoma: a 2017 update. Hepatology International, 2017, 11, 317-370.	4.2	1,537
153	Diagnostic Performance of Gadoxetic Acid–enhanced Liver MR Imaging versus Multidetector CT in the Detection of Dysplastic Nodules and Early Hepatocellular Carcinoma. Radiology, 2017, 285, 134-146.	7.3	78
154	Value of MR elastography for the preoperative estimation of liver regeneration capacity in patients with hepatocellular carcinoma. Journal of Magnetic Resonance Imaging, 2017, 45, 1627-1636.	3.4	18
155	Nucleos(t)ide Analogue Treatment for Patients With Hepatitis B Virus (HBV) e Antigen–Positive Chronic HBV Genotype C Infection: A Nationwide, Multicenter, Retrospective Study. Journal of Infectious Diseases, 2017, 216, 1407-1414.	4.0	33
156	Primary malignant tumours in the non-cirrhotic liver. European Journal of Radiology, 2017, 95, 349-361.	2.6	52
157	Comparative characteristics of quantitative indexes for 18F-FDG uptake and metabolic volume in sequentially obtained PET/MRI and PET/CT. Nuclear Medicine Communications, 2017, 38, 333-339.	1.1	1
158	Old and New MR Tools to Measure Hepatic Steatosis: Is Their Diagnostic Accuracy the Same?. Radiology, 2017, 284, 303-304.	7.3	0
159	Clinical Feasibility of Free-Breathing Dynamic T1-Weighted Imaging With Gadoxetic Acid–Enhanced Liver Magnetic Resonance Imaging Using a Combination of Variable Density Sampling and Compressed Sensing. Investigative Radiology, 2017, 52, 596-604.	6.2	29
160	Clinical Feasibility of 3-Dimensional Magnetic Resonance Cholangiopancreatography Using Compressed Sensing. Investigative Radiology, 2017, 52, 612-619.	6.2	66
161	Magnetic resonance imaging evaluation of the distal oblique bundle in the distal interosseous membrane of the forearm. BMC Musculoskeletal Disorders, 2017, 18, 47.	1.9	13
162	Preoperative Assessment of Pancreatic Cancer with FDG PET/MR Imaging versus FDG PET/CT Plus Contrast-enhanced Multidetector CT: A Prospective Preliminary Study. Radiology, 2017, 282, 149-159.	7.3	74

#	Article	IF	CITATIONS
163	Hepatic stiffness measurement by using MR elastography: prognostic values after hepatic resection for hepatocellular carcinoma. European Radiology, 2017, 27, 1713-1721.	4.5	41
164	Liver imaging reporting and data system v2014 categorization of hepatocellular carcinoma on gadoxetic acidâ€enhanced MRI: Comparison with multiphasic multidetector computed tomography. Journal of Magnetic Resonance Imaging, 2017, 45, 731-740.	3.4	55
165	Real-time US-CT/MR fusion imaging for percutaneous radiofrequency ablation of hepatocellular carcinoma. Journal of Hepatology, 2017, 66, 347-354.	3.7	103
166	Quantitative Liver Function Analysis: Volumetric T1 Mapping with Fast Multisection B ₁ Inhomogeneity Correction in Hepatocyte-specific Contrast-enhanced Liver MR Imaging. Radiology, 2017, 282, 408-417.	7.3	65
167	Thermal Injury–induced Hepatic Parenchymal Hypoperfusion: Risk of Hepatocellular Carcinoma Recurrence after Radiofrequency Ablation. Radiology, 2017, 282, 880-891.	7.3	16
168	Comparison of biannual ultrasonography and annual non-contrast liver magnetic resonance imaging as surveillance tools for hepatocellular carcinoma in patients with liver cirrhosis (MAGNUS-HCC): a study protocol. BMC Cancer, 2017, 17, 877.	2.6	30
169	Prospective Validation of Intra- and Interobserver Reproducibility of a New Point Shear Wave Elastographic Technique for Assessing Liver Stiffness in Patients with Chronic Liver Disease. Korean Journal of Radiology, 2017, 18, 926.	3.4	21
170	Diagnosis of Hepatocellular Carcinoma with Gadoxetic Acid-Enhanced MRI: 2016 Consensus Recommendations of the Korean Society of Abdominal Radiology. Korean Journal of Radiology, 2017, 18, 427.	3.4	42
171	T2* Mapping from Multi-Echo Dixon Sequence on Gadoxetic Acid-Enhanced Magnetic Resonance Imaging for the Hepatic Fat Quantification: Can It Be Used for Hepatic Function Assessment?. Korean Journal of Radiology, 2017, 18, 682.	3.4	7
172	Liver fibrosis staging with a new 2D-shear wave elastography using comb-push technique: Applicability, reproducibility, and diagnostic performance. PLoS ONE, 2017, 12, e0177264.	2.5	31
173	Pancreatic Tumors. Medical Radiology, 2017, , 491-525.	0.1	0
174	No-Touch Radiofrequency Ablation: A Comparison of Switching Bipolar and Switching Monopolar Ablation inEx VivoBovine Liver. Korean Journal of Radiology, 2017, 18, 279.	3.4	25
175	Percutaneous Dual-Switching Monopolar Radiofrequency Ablation Using a Separable Clustered Electrode: A Preliminary Study. Korean Journal of Radiology, 2017, 18, 799.	3.4	12
176	Ultrasound-guided percutaneous portal transplantation of peripheral blood monocytes in patients with liver cirrhosis. Korean Journal of Internal Medicine, 2017, 32, 261-268.	1.7	8
177	No-touch radiofrequency ablation using multiple electrodes: An in vivo comparison study of switching monopolar versus switching bipolar modes in porcine livers. PLoS ONE, 2017, 12, e0176350.	2.5	20
178	Imaging Diagnosis of Pancreatic Cancer: CT and MRI. , 2017, , 95-114.		1
179	Prospective Comparison of Liver Stiffness Measurements between Two Point Shear Wave Elastography Methods: Virtual Touch Quantification and Elastography Point Quantification. Korean Journal of Radiology, 2016, 17, 750.	3.4	20
180	Triple Arterial Phase MR Imaging with Gadoxetic Acid Using a Combination of Contrast Enhanced Time Robust Angiography, Keyhole, and Viewsharing Techniques and Two-Dimensional Parallel Imaging in Comparison with Conventional Single Arterial Phase. Korean Journal of Radiology, 2016, 17, 522.	3.4	29

#	Article	IF	CITATIONS
181	Noninvasive Diagnosis of Hepatocellular Carcinoma: Elaboration on Korean Liver Cancer Study Group-National Cancer Center Korea Practice Guidelines Compared with Other Guidelines and Remaining Issues. Korean Journal of Radiology, 2016, 17, 7.	3.4	48
182	Clinical Utility of Liver Stiffness Measurements on Magnetic Resonance Elastrography in Patients with Hepatocellular Carcinoma Treated with Radiofrequency Ablation. Investigative Magnetic Resonance Imaging, 2016, 20, 231.	0.4	1
183	Comparison of Multidetector CT and Gadobutrol-Enhanced MR Imaging for Evaluation of Small, Solid Pancreatic Lesions. Korean Journal of Radiology, 2016, 17, 509.	3.4	13
184	Diagnostic accuracy of liver imaging reporting and data system (Llâ€RADS) v2014 for intrahepatic massâ€forming cholangiocarcinomas in patients with chronic liver disease on gadoxetic acidâ€enhanced MRI. Journal of Magnetic Resonance Imaging, 2016, 44, 1330-1338.	3.4	67
185	Multiphasic Dynamic Computed Tomography Evaluation of Liver Tissue Perfusion Characteristics Using the Dual Maximum Slope Model in Patients With Cirrhosis and Hepatocellular Carcinoma. Investigative Radiology, 2016, 51, 430-434.	6.2	14
186	Comparison of Knowledge-based Iterative Model Reconstruction and Hybrid Reconstruction Techniques for Liver CT Evaluation of Hypervascular Hepatocellular Carcinoma. Journal of Computer Assisted Tomography, 2016, 40, 863-871.	0.9	21
187	Health economic evaluation of Gd-EOB-DTPA MRI vs ECCM-MRI and multi-detector computed tomography in patients with suspected hepatocellular carcinoma in Thailand and South Korea. Journal of Medical Economics, 2016, 19, 759-768.	2.1	14
188	Colorectal Cancer Liver Metastases: Diagnostic Performance and Prognostic Value of PET/MR Imaging. Radiology, 2016, 280, 782-792.	7.3	58
189	Pre-treatment estimation of future remnant liver function using gadoxetic acid MRI in patients with HCC. Journal of Hepatology, 2016, 65, 1155-1162.	3.7	41
190	Recent Advances in the Imaging Diagnosis of Hepatocellular Carcinoma: Value of Gadoxetic Acid-Enhanced MRI. Liver Cancer, 2016, 5, 67-87.	7.7	68
191	Percutaneous ethanol injection therapy is comparable to radiofrequency ablation in hepatocellular carcinoma smaller than 1.5 cm. Medicine (United States), 2016, 95, e4551.	1.0	13
192	Diffusion-Related MRI Parameters for Assessing Early Treatment Response of Liver Metastases to Cytotoxic Therapy in Colorectal Cancer. American Journal of Roentgenology, 2016, 207, W26-W32.	2.2	36
193	Portal Vein Thrombosis in Patients with Hepatocellular Carcinoma: Diagnostic Accuracy of Gadoxetic Acid–enhanced MR Imaging. Radiology, 2016, 279, 773-783.	7.3	35
194	Differentiation of intrahepatic mass-forming cholangiocarcinoma from hepatocellular carcinoma on gadoxetic acid-enhanced liver MR imaging. European Radiology, 2016, 26, 1808-1817.	4.5	73
195	25 Years of Contrast-Enhanced MRI: Developments, Current Challenges and Future Perspectives. Advances in Therapy, 2016, 33, 1-28.	2.9	297
196	Liver Fibrosis Staging with MR Elastography: Comparison of Diagnostic Performance between Patients with Chronic Hepatitis B and Those with Other Etiologic Causes. Radiology, 2016, 280, 88-97.	7.3	54
197	Assessment of the association between Apgar scores and seizures in infants less than 1 year old. Seizure: the Journal of the British Epilepsy Association, 2016, 37, 48-54.	2.0	9
198	Added Value of Integrated Whole-Body PET/MRI for Evaluation of Colorectal Cancer: Comparison With Contrast-Enhanced MDCT. American Journal of Roentgenology, 2016, 206, W10-W20.	2.2	64

#	Article	IF	CITATIONS
199	Body Diffusion-weighted MR Imaging in Oncology. Magnetic Resonance Imaging Clinics of North America, 2016, 24, 31-44.	1.1	17
200	Pancreatic Steatosis and Fibrosis: Quantitative Assessment with Preoperative Multiparametric MR Imaging. Radiology, 2016, 279, 140-150.	7.3	88
201	Assessment of Malignant Potential in Intraductal Papillary Mucinous Neoplasms of the Pancreas: Comparison between Multidetector CT and MR Imaging with MR Cholangiopancreatography. Radiology, 2016, 279, 128-139.	7.3	54
202	Monitoring Vascular Disrupting Therapy in a Rabbit Liver Tumor Model: Relationship between Tumor Perfusion Parameters at IVIM Diffusion-weighted MR Imaging and Those at Dynamic Contrast-enhanced MR Imaging. Radiology, 2016, 278, 104-113.	7.3	37
203	Pancreatic neuroendocrine tumour (PNET): Staging accuracy of MDCT and its diagnostic performance for the differentiation of PNET with uncommon CT findings from pancreatic adenocarcinoma. European Radiology, 2016, 26, 1338-1347.	4.5	71
204	Quantitative assessment of hepatic function: modified look-locker inversion recovery (MOLLI) sequence for T1 mapping on Gd-EOB-DTPA-enhanced liver MR imaging. European Radiology, 2016, 26, 1775-1782.	4.5	69
205	Hepatic Steatosis: Assessment with Acoustic Structure Quantification of US Imaging. Radiology, 2016, 278, 257-264.	7.3	60
206	Consensus report from the 7th International Forum for Liver Magnetic Resonance Imaging. European Radiology, 2016, 26, 674-682.	4.5	86
207	Switching Monopolar Radiofrequency Ablation Using a Separable Cluster Electrode in Patients with Hepatocellular Carcinoma: A Prospective Study. PLoS ONE, 2016, 11, e0161980.	2.5	14
208	Prospective comparison of 3T MRI with diffusionâ€weighted imaging and MDCT for the preoperative TNM staging of gastric cancer. Journal of Magnetic Resonance Imaging, 2015, 41, 814-821.	3.4	64
209	Imaging of IPMN of the pancreas: evaluation of malignant potential and resectability. Cancer Imaging, 2015, 15, .	2.8	0
210	Clinical Performance of Whole-Body 18F-FDG PET/Dixon-VIBE, T1-Weighted, and T2-Weighted MRI Protocol in Colorectal Cancer. Clinical Nuclear Medicine, 2015, 40, e392-e398.	1.3	17
211	2014 Korean Liver Cancer Study Group-National Cancer Center Korea Practice Guideline for the Management of Hepatocellular Carcinoma. Korean Journal of Radiology, 2015, 16, 465.	3.4	168
212	Integrated Whole Body MR/PET: Where Are We?. Korean Journal of Radiology, 2015, 16, 32.	3.4	44
213	Heterogeneous living donor hepatic fat distribution on MRI chemical shift imaging. Annals of Surgical Treatment and Research, 2015, 89, 37.	1.0	14
214	Cancer Stem Cells in Primary Liver Cancers: Pathological Concepts and Imaging Findings. Korean Journal of Radiology, 2015, 16, 50.	3.4	37
215	Dynamic Contrast-Enhanced MRI Using a Macromolecular MR Contrast Agent (P792): Evaluation of Antivascular Drug Effect in a Rabbit VX2 Liver Tumor Model. Korean Journal of Radiology, 2015, 16, 1029.	3.4	6
216	Reduced Field-of-View Diffusion-Weighted Magnetic Resonance Imaging of the Pancreas: Comparison with Conventional Single-Shot Echo-Planar Imaging. Korean Journal of Radiology, 2015, 16, 1216.	3.4	50

#	Article	IF	CITATIONS
217	Pulmonary Nodule Detection in Patients with a Primary Malignancy Using Hybrid PET/MRI: Is There Value in Adding Contrast-Enhanced MR Imaging?. PLoS ONE, 2015, 10, e0129660.	2.5	13
218	Gadoxetic acid-enhanced MRI and diffusion-weighted imaging for the detection of colorectal liver metastases after neoadjuvant chemotherapy. European Radiology, 2015, 25, 2428-2436.	4.5	21
219	Fat-suppressed, three-dimensional T1-weighted imaging using high-acceleration parallel acquisition and a dual-echo Dixon technique for gadoxetic acid-enhanced liver MRI at 3 T. Acta Radiologica, 2015, 56, 1454-1462.	1.1	7
220	Leiomyomas in the gastric cardia: CT findings and differentiation from gastrointestinal stromal tumors. European Journal of Radiology, 2015, 84, 1694-1700.	2.6	23
221	Initial Performance of Radiologists and Radiology Residents in Interpreting Low-Dose (2-mSv) Appendiceal CT. American Journal of Roentgenology, 2015, 205, W594-W611.	2.2	15
222	Novel Imaging Diagnosis for Hepatocellular Carcinoma: Consensus from the 5th Asia-Pacific Primary Liver Cancer Expert Meeting (APPLE 2014). Liver Cancer, 2015, 4, 215-227.	7.7	14
223	Diagnostic Performance of Gadoxetic Acid–enhanced Liver MR Imaging in the Detection of HCCs and Allocation of Transplant Recipients on the Basis of the Milan Criteria and UNOS Guidelines: Correlation with Histopathologic Findings. Radiology, 2015, 274, 149-160.	7.3	41
224	Hepatocellular Carcinoma: Diagnostic Performance of Multidetector CT and MR Imaging—A Systematic Review and Meta-Analysis. Radiology, 2015, 275, 97-109.	7.3	393
225	Influence of the adaptive iterative dose reduction 3D algorithm on the detectability of low-contrast lesions and radiation dose repeatability in abdominal computed tomography: a phantom study. Abdominal Imaging, 2015, 40, 1843-1852.	2.0	8
226	Prediction of microvascular invasion of hepatocellular carcinoma using gadoxetic acid-enhanced MR and 18F-FDG PET/CT. Abdominal Imaging, 2015, 40, 843-851.	2.0	98
227	Intraductal Papillary Mucinous Neoplasms of the Pancreas: Evaluation of Malignant Potential and Surgical Resectability by Using MR Imaging with MR Cholangiography. Radiology, 2015, 274, 723-733.	7.3	39
228	Hybrid iterative reconstruction technique for liver CT scans for image noise reduction and image quality improvement: evaluation of the optimal iterative reconstruction strengths. Radiologia Medica, 2015, 120, 259-267.	7.7	17
229	Navigated three-dimensional T1-weighted gradient-echo sequence for gadoxetic acid liver magnetic resonance imaging in patients with limited breath-holding capacity. Abdominal Imaging, 2015, 40, 278-288.	2.0	14
230	Switching bipolar hepatic radiofrequency ablation using internally cooled wet electrodes: comparison with consecutive monopolar and switching monopolar modes. British Journal of Radiology, 2015, 88, 20140468.	2.2	26
231	Diagnosing Borderline Hepatic Nodules in Hepatocarcinogenesis: Imaging Performance. American Journal of Roentgenology, 2015, 205, 10-21.	2.2	38
232	Non-hypervascular hepatobiliary phase hypointense nodules on gadoxetic acid-enhanced MRI: Risk of HCC recurrence after radiofrequency ablation. Journal of Hepatology, 2015, 62, 1122-1130.	3.7	70
233	Effect of muscle mass on toxicity and survival in patients with colon cancer undergoing adjuvant chemotherapy. Supportive Care in Cancer, 2015, 23, 687-694.	2.2	178
234	Combined Use of MR Fat Quantification and MR Elastography in Living Liver Donors: Can It Reduce the Need for Preoperative Liver Biopsy?. Radiology, 2015, 276, 453-464.	7.3	44

#	Article	IF	CITATIONS
235	Estimation of Hepatic Extracellular Volume Fraction Using Multiphasic Liver Computed Tomography for Hepatic Fibrosis Grading. Investigative Radiology, 2015, 50, 290-296.	6.2	70
236	Noninvasive diagnosis of hepatocellular carcinoma on gadoxetic acid-enhanced MRI: can hypointensity on the hepatobiliary phase be used as an alternative to washout?. European Radiology, 2015, 25, 2859-2868.	4.5	117
237	Evaluation of Perihilar Biliary Strictures: Does DWI Provide Additional Value to Conventional MRI?. American Journal of Roentgenology, 2015, 205, 789-796.	2.2	15
238	Feasibility of three-dimensional virtual surgical planning in living liver donors. Abdominal Imaging, 2015, 40, 510-520.	2.0	12
239	Dynamic contrastâ€enhanced MRI of gastric cancer: Correlation of the perfusion parameters with pathological prognostic factors. Journal of Magnetic Resonance Imaging, 2015, 41, 1608-1614.	3.4	21
240	Preoperative staging of gallbladder carcinoma using biliary MR imaging. Journal of Magnetic Resonance Imaging, 2015, 41, 314-321.	3.4	24
241	Differentiation of poorly differentiated colorectal adenocarcinomas from well- or moderately differentiated colorectal adenocarcinomas at contrast-enhanced multidetector CT. Abdominal Imaging, 2015, 40, 1-10.	2.0	20
242	Differentiation of lipid poor angiomyolipoma from hepatocellular carcinoma on gadoxetic acid-enhanced liver MR imaging. Abdominal Imaging, 2015, 40, 531-541.	2.0	27
243	Clinical Implication of Anti-Angiogenic Effect of Regorafenib in Metastatic Colorectal Cancer. PLoS ONE, 2015, 10, e0145004.	2.5	20
244	Neoplasms of the Gallbladder and Biliary Tract. , 2015, , 1402-1426.		0
245	Two Cases of Diabetic Ketoacidosis Associated with Paliperidone Treatment in Schizophrenia. Journal of Korean Diabetes, 2014, 15, 178.	0.3	0
246	Noninvasive Assessment of Hepatic Fibrosis in Patients with Chronic Hepatitis B Viral Infection Using Magnetic Resonance Elastography. Korean Journal of Radiology, 2014, 15, 210.	3.4	31
247	Adaptive Iterative Dose Reduction Algorithm in CT: Effect on Image Quality Compared with Filtered Back Projection in Body Phantoms of Different Sizes. Korean Journal of Radiology, 2014, 15, 195.	3.4	35
248	Monopolar Radiofrequency Ablation Using a Dual-Switching System and a Separable Clustered Electrode: Evaluation of the <i>In Vivo</i> Efficiency. Korean Journal of Radiology, 2014, 15, 235.	3.4	24
249	Shear Wave Elastography for Liver Stiffness Measurement in Clinical Sonographic Examinations. Journal of Ultrasound in Medicine, 2014, 33, 437-447.	1.7	85
250	2014 KLCSG-NCC Korea Practice Guidelines for the Management of Hepatocellular Carcinoma: HCC Diagnostic Algorithm. Digestive Diseases, 2014, 32, 764-777.	1.9	60
251	Metastatic testicular tumor presenting as a scrotal hydrocele: An initial manifestation of pancreatic adenocarcinoma. Oncology Letters, 2014, 7, 1793-1795.	1.8	9

252 Imaging and quantification of fatty liver by terahertz wave. , 2014, , .

#	Article	IF	CITATIONS
253	Non-Hypervascular Hypointense Nodules ≥1 cm on the Hepatobiliary Phase of Gadoxetic Acid-Enhanced Magnetic Resonance Imaging in Cirrhotic Livers. Digestive Diseases, 2014, 32, 678-689.	1.9	26
254	Intravoxel Incoherent Motion Diffusion-weighted MR Imaging of Hepatocellular Carcinoma: Correlation with Enhancement Degree and Histologic Grade. Radiology, 2014, 270, 758-767.	7.3	175
255	Small Single-Nodule Hepatocellular Carcinoma: Comparison of Transarterial Chemoembolization, Radiofrequency Ablation, and Hepatic Resection by Using Inverse Probability Weighting. Radiology, 2014, 271, 909-918.	7.3	97
256	Ultra-low Peak Voltage CT Colonography: Effect of Iterative Reconstruction Algorithms on Performance of Radiologists Who Use Anthropomorphic Colonic Phantoms. Radiology, 2014, 273, 759-771.	7.3	16
257	Intravoxel Incoherent Motion Diffusion-weighted MR Imaging for Monitoring the Therapeutic Efficacy of the Vascular Disrupting Agent CKD-516 in Rabbit VX2 Liver Tumors. Radiology, 2014, 272, 417-426.	7.3	80
258	Nonalcoholic Fatty Liver Disease: Intravoxel Incoherent Motion Diffusion-weighted MR Imaging—An Experimental Study in a Rabbit Model. Radiology, 2014, 270, 131-140.	7.3	57
259	Hepatic Fibrosis: Prospective Comparison of MR Elastography and US Shear-Wave Elastography for Evaluation. Radiology, 2014, 273, 772-782.	7.3	147
260	Consensus report from the 6th International forum for liver MRI using gadoxetic acid. Journal of Magnetic Resonance Imaging, 2014, 40, 516-529.	3.4	40
261	Intravoxel Incoherent Motion Diffusion-Weighted Imaging of Pancreatic Neuroendocrine Tumors. Investigative Radiology, 2014, 49, 396-402.	6.2	48
262	MR elastography for noninvasive assessment of hepatic fibrosis: Reproducibility of the examination and reproducibility and repeatability of the liver stiffness value measurement. Journal of Magnetic Resonance Imaging, 2014, 39, 326-331.	3.4	93
263	Radiofrequency Ablation for Intrahepatic Recurrent Hepatocellular Carcinoma: Long-Term Results and Prognostic Factors in 168 Patients with Cirrhosis. CardioVascular and Interventional Radiology, 2014, 37, 705-715.	2.0	28
264	High-resolution T1-weighted gradient echo imaging for liver MRI using parallel imaging at high-acceleration factors. Abdominal Imaging, 2014, 39, 711-721.	2.0	14
265	Evaluation of hepatic focal lesions using diffusionâ€weighted MR imaging: Comparison of apparent diffusion coefficient and intravoxel incoherent motionâ€derived parameters. Journal of Magnetic Resonance Imaging, 2014, 39, 276-285.	3.4	93
266	Usefulness of MR elastography for predicting esophageal varices in cirrhotic patients. Journal of Magnetic Resonance Imaging, 2014, 39, 559-566.	3.4	32
267	Diffuse Liver Disease. Radiology Illustrated, 2014, , 21-73.	0.0	0
268	Differential diagnosis of benign and malignant distal biliary strictures: Value of adding diffusion-weighted imaging to conventional magnetic resonance cholangiopancreatography. Journal of Magnetic Resonance Imaging, 2014, 39, 1509-1517.	3.4	13
269	MRI Features of Gastrointestinal Stromal Tumors. American Journal of Roentgenology, 2014, 203, 980-991.	2.2	63
270	Postablation Assessment Using Follow-Up Registration of CT Images Before and After Radiofrequency Ablation (RFA): Prospective Evaluation of Midterm Therapeutic Results of RFA for Hepatocellular Carcinoma. American Journal of Roentgenology, 2014, 203, 70-77.	2.2	32

#	Article	IF	CITATIONS
271	Hepatic Steatosis in Living Liver Donor Candidates: Preoperative Assessment by Using Breath-hold Triple-Echo MR Imaging and ¹ H MR Spectroscopy. Radiology, 2014, 271, 730-738.	7.3	50
272	Dynamic contrast-enhanced MRI to evaluate the therapeutic response to neoadjuvant chemoradiation therapy in locally advanced rectal cancer. Journal of Magnetic Resonance Imaging, 2014, 40, 730-737.	3.4	64
273	CT and MR Imaging Diagnosis and Staging of Hepatocellular Carcinoma: Part II. Extracellular Agents, Hepatobiliary Agents, and Ancillary Imaging Features. Radiology, 2014, 273, 30-50.	7.3	430
274	CT and MR Imaging Diagnosis and Staging of Hepatocellular Carcinoma: Part I. Development, Growth, and Spread: Key Pathologic and Imaging Aspects. Radiology, 2014, 272, 635-654.	7.3	401
275	Prediction of Esophageal Varices in Patients with Cirrhosis: Usefulness of Three-dimensional MR Elastography with Echo-planar Imaging Technique. Radiology, 2014, 272, 143-153.	7.3	97
276	In-Service Education and Training for Teachers in Korea and the Role of the Private Sector from 1945 to 1970s. Asia-Pacific Education Researcher, 2014, 23, 413-424.	3.7	0
277	Prediction of aggressiveness in early-stage hepatocellular carcinoma for selection of surgical resection. Journal of Hepatology, 2014, 60, 1219-1224.	3.7	39
278	High-intensity Focused Ultrasound Ablation of Soft-tissue Tumors and Assessment of Treatment Response with Multiparametric Magnetic Resonance Imaging: Preliminary Study Using Rabbit VX2 Tumor Model. Journal of Medical Ultrasound, 2014, 22, 99-105.	0.4	4
279	Radiofrequency Ablation of Hepatocellular Carcinoma as First-Line Treatment: Long-term Results and Prognostic Factors in 162 Patients with Cirrhosis. Radiology, 2014, 270, 900-909.	7.3	256
280	Intravoxel Incoherent Motion Diffusion-weighted MR Imaging for Characterization of Focal Pancreatic Lesions. Radiology, 2014, 270, 444-453.	7.3	146
281	Imaging diagnosis of pancreatic cancer: A state-of-the-art review. World Journal of Gastroenterology, 2014, 20, 7864.	3.3	297
282	Comparison of Iterative Model–Based Reconstruction Versus Conventional Filtered Back Projection and Hybrid Iterative Reconstruction Techniques. Journal of Computer Assisted Tomography, 2014, 38, 859-868.	0.9	24
283	Evaluation of Hepatic Fibrosis Using Intravoxel Incoherent Motion in Diffusion-Weighted Liver MRI. Journal of Computer Assisted Tomography, 2014, 38, 110-116.	0.9	82
284	Liver Computed Tomography With Low Tube Voltage and Model-Based Iterative Reconstruction Algorithm for Hepatic Vessel Evaluation in Living Liver Donor Candidates. Journal of Computer Assisted Tomography, 2014, 38, 367-375.	0.9	16
285	High Spatial Resolution, Respiratory-Gated, T1-Weighted Magnetic Resonance Imaging of the Liver and the Biliary Tract During the Hepatobiliary Phase of Gadoxetic Acid–Enhanced Magnetic Resonance Imaging. Journal of Computer Assisted Tomography, 2014, 38, 360-366.	0.9	21
286	Quantification of the Fat Fraction in the Liver Using Dual-Energy Computed Tomography and Multimaterial Decomposition. Journal of Computer Assisted Tomography, 2014, 38, 845-852.	0.9	42
287	Magnetic Resonance Imaging Spectrum of Solid Pseudopapillary Neoplasm of the Pancreas. Journal of Computer Assisted Tomography, 2014, 38, 249-257.	0.9	7
288	Early quantification of the therapeutic efficacy of the vascular disrupting agent, CKD-516, using dynamic contrast-enhanced ultrasonography in rabbit VX2 liver tumors. Ultrasonography, 2014, 33, 18-25.	2.3	10

#	Article	IF	CITATIONS
289	State-of-the-art preoperative staging of gastric cancer by MDCT and magnetic resonance imaging. World Journal of Gastroenterology, 2014, 20, 4546.	3.3	56
290	MR Imaging of Hepatocellular Carcinoma. , 2014, , 169-207.		0
291	Consensus Report of the Fifth International Forum for Liver MRI. American Journal of Roentgenology, 2013, 201, 97-107.	2.2	38
292	Imaging bile duct tumors: pathologic concepts, classification, and early tumor detection. Abdominal Imaging, 2013, 38, 1334-1350.	2.0	51
293	Free-breathing dynamic contrast-enhanced MRI of the abdomen and chest using a radial gradient echo sequence with K-space weighted image contrast (KWIC). European Radiology, 2013, 23, 1352-1360.	4.5	52
294	Intraductal Papillary Mucinous Neoplasms With Associated Invasive Carcinoma of the Pancreas: Imaging Findings and Diagnostic Performance of MDCT for Prediction of Prognostic Factors. American Journal of Roentgenology, 2013, 201, 565-572.	2.2	18
295	Solid Pancreatic Lesions: Characterization by Using Timing Bolus Dynamic Contrast-enhanced MR Imaging Assessment—A Preliminary Study. Radiology, 2013, 266, 185-196.	7.3	74
296	Estimation of saline-mixed tissue conductivity and ablation lesion size. Computers in Biology and Medicine, 2013, 43, 504-512.	7.0	14
297	Vascular disrupting effect of CKD-516: preclinical study using DCE-MRI. Investigational New Drugs, 2013, 31, 1097-1106.	2.6	29
298	Small- and Medium-sized Hepatocellular Carcinomas: Monopolar Radiofrequency Ablation with a Multiple-Electrode Switching System—Mid-term Results. Radiology, 2013, 268, 589-600.	7.3	51
299	Hepatocellular Carcinoma: Imaging Patterns on Gadoxetic Acid–enhanced MR Images and Their Value as an Imaging Biomarker. Radiology, 2013, 267, 776-786.	7.3	154
300	Diagnostic Performance of MDCT for Predicting Important Prognostic Factors in Pancreatic Cancer. Pancreas, 2013, 42, 1316-1322.	1.1	13
301	Comparison of Magnetic Resonance Elastography and Gadoxetate Disodium–Enhanced Magnetic Resonance Imaging for the Evaluation of Hepatic Fibrosis. Investigative Radiology, 2013, 48, 607-613.	6.2	45
302	Serum Insulin-like Growth Factor-I Level Is an Independent Predictor of Recurrence and Survival in Early Hepatocellular Carcinoma: A Prospective Cohort Study. Clinical Cancer Research, 2013, 19, 4218-4227.	7.0	28
303	Low Tube Voltage Intermediate Tube Current Liver MDCT: Sinogram-Affirmed Iterative Reconstruction Algorithm for Detection of Hypervascular Hepatocellular Carcinoma. American Journal of Roentgenology, 2013, 201, 23-32.	2.2	55
304	Assessment of a Model-Based, Iterative Reconstruction Algorithm (MBIR) Regarding Image Quality and Dose Reduction in Liver Computed Tomography. Investigative Radiology, 2013, 48, 598-606.	6.2	119
305	Added value of diffusionâ€weighted imaging to MR cholangiopancreatography with unenhanced mr imaging for predicting malignancy or invasiveness of intraductal papillary mucinous neoplasm of the pancreas. Journal of Magnetic Resonance Imaging, 2013, 38, 555-563.	3.4	57
306	Clinical application of controlled aliasing in parallel imaging results in a higher acceleration (CAIPIRINHA)â€volumetric interpolated breathhold (VIBE) sequence for gadoxetic acidâ€enhanced liver MR imaging. Journal of Magnetic Resonance Imaging, 2013, 38, 1020-1026.	3.4	54

#	Article	IF	CITATIONS
307	Role of diffusion-weighted magnetic resonance imaging in the diagnosis of gallbladder cancer. Journal of Magnetic Resonance Imaging, 2013, 38, 127-137.	3.4	39
308	MR elastography of healthy liver parenchyma: Normal value and reliability of the liver stiffness value measurement. Journal of Magnetic Resonance Imaging, 2013, 38, 1215-1223.	3.4	80
309	Gadoxetic acid-enhanced MRI with MR cholangiography for the preoperative evaluation of bile duct cancer. Journal of Magnetic Resonance Imaging, 2013, 38, 138-147.	3.4	20
310	The Right Posterior Bile Duct Anatomy of the Donor Is Important in Biliary Complications of the Recipients After Living-Donor Liver Transplantation. Annals of Surgery, 2013, 257, 702-707.	4.2	30
311	Iterative Reconstruction Algorithms of Computed Tomography for the Assessment of Small Pancreatic Lesions. Journal of Computer Assisted Tomography, 2013, 37, 911-923.	0.9	11
312	Staging of Hepatic Fibrosis: Comparison of Magnetic Resonance Elastography and Shear Wave Elastography in the Same Individuals. Korean Journal of Radiology, 2013, 14, 202.	3.4	67
313	Dual Switching Monopolar Radiofrequency Ablation Using a Separable Clustered Electrode: Comparison with Consecutive and Switching Monopolar Modes in <i>Ex Vivo</i> Bovine Livers. Korean Journal of Radiology, 2013, 14, 403.	3.4	19
314	Evaluation of theln VivoEfficiency and Safety of Hepatic Radiofrequency Ablation Using a 15-G Octopus® in Pig Liver. Korean Journal of Radiology, 2013, 14, 194.	3.4	10
315	Detection of Recurrent Hepatocellular Carcinoma in Cirrhotic Liver after Transcatheter Arterial Chemoembolization: Value of Quantitative Color Mapping of the Arterial Enhancement Fraction of the Liver. Korean Journal of Radiology, 2013, 14, 51.	3.4	16
316	MR Imaging in Patients with Suspected Liver Metastases: Value of Liver-Specific Contrast Agent Gadoxetic Acid. Korean Journal of Radiology, 2013, 14, 894.	3.4	53
317	Initial Assessment of Dual-Energy CT in Patients With Gallstones or Bile Duct Stones: Can Virtual Nonenhanced Images Replace True Nonenhanced Images?. American Journal of Roentgenology, 2012, 198, 817-824.	2.2	34
318	Intrahepatic Mass-forming Cholangiocarcinoma: Enhancement Patterns on Gadoxetic Acid–enhanced MR Images. Radiology, 2012, 264, 751-760.	7.3	162
319	Feasibility and Accuracy of Dual-Source Dual-Energy CT for Noninvasive Determination of Hepatic Iron Accumulation. Radiology, 2012, 262, 126-135.	7.3	68
320	Detection of Small (â‰ 2 0 mm) Pancreatic Adenocarcinoma: Histologic Grading and CT Enhancement Features. Radiology, 2012, 262, 1044-1045.	7.3	6
321	Enhancement patterns of hepatocellular carcinomas on multiphasic multidetector row CT: comparison with pathological differentiation. British Journal of Radiology, 2012, 85, e573-e583.	2.2	88
322	Multiple-electrode radiofrequency ablations using Octopus® electrodes in an <i>in vivo</i> porcine liver model. British Journal of Radiology, 2012, 85, e609-e615.	2.2	15
323	Lymph Node Metastases from Gastric Cancer: Gadofluorine M and Gadopentetate Dimeglumine MR Imaging in a Rabbit Model. Radiology, 2012, 263, 391-400.	7.3	9
324	Recent Advances in CT and MR Imaging for Evaluation of Hepatocellular Carcinoma. Liver Cancer, 2012, 1, 22-40.	7.7	62

#	Article	IF	CITATIONS
325	Attenuation-based Automatic Tube Voltage Selection and Tube Current Modulation for Dose Reduction at Contrast-enhanced Liver CT. Radiology, 2012, 265, 437-447.	7.3	92
326	Imaging Findings of Cirrhotic Liver. Medical Radiology, 2012, , 47-83.	0.1	0
327	Adaptive Statistical Iterative Reconstruction and Veo. Journal of Computer Assisted Tomography, 2012, 36, 596-601.	0.9	43
328	Dual-source, dual-energy multidetector CT for the evaluation of pancreatic tumours. British Journal of Radiology, 2012, 85, e891-e898.	2.2	55
329	Clinical and Duplex-Sonographic Outcomes of 1,320-nm Endovenous Laser Treatment for Saphenous Vein Incompetence. Dermatologic Surgery, 2012, 38, 1704-1709.	0.8	5
330	Preoperative assessment of longitudinal extent of bile duct cancers using MDCT with multiplanar reconstruction and minimum intensity projections: Comparison with MR cholangiography. European Journal of Radiology, 2012, 81, 2020-2026.	2.6	17
331	Diagnosis of Hepatocellular Carcinoma: Newer Radiological Tools. Seminars in Oncology, 2012, 39, 399-409.	2.2	61
332	Two-way actuation behavior of shape memory polymer/elastomer core/shell composites. Smart Materials and Structures, 2012, 21, 035028.	3.5	44
333	80-kVp CT Using Iterative Reconstruction in Image Space Algorithm for the Detection of Hypervascular Hepatocellular Carcinoma: Phantom and Initial Clinical Experience. Korean Journal of Radiology, 2012, 13, 152.	3.4	44
334	Percutaneous Radiofrequency Ablation with Multiple Electrodes for Medium-Sized Hepatocellular Carcinomas. Korean Journal of Radiology, 2012, 13, 34.	3.4	57
335	Evaluation of lymph node metastases: Comparison of gadofluorine Mâ€enhanced MRI and diffusionâ€weighted MRI in a rabbit VX2 rectal cancer model. Journal of Magnetic Resonance Imaging, 2012, 35, 1179-1186.	3.4	5
336	Magnetic resonance imaging findings of the massâ€forming type of autoimmune pancreatitis: Comparison with pancreatic adenocarcinoma. Journal of Magnetic Resonance Imaging, 2012, 36, 188-197.	3.4	95
337	Quantification of hepatic macrosteatosis in living, related liver donors using T1â€independent, T2*â€corrected chemical shift MRI. Journal of Magnetic Resonance Imaging, 2012, 36, 1124-1130.	3.4	25
338	Prognostic implications of tumor vascularity and its relationship to cytokeratin 19 expression in patients with hepatocellular carcinoma. Abdominal Imaging, 2012, 37, 439-446.	2.0	19
339	Comparison of Semiautomated and Manual Measurements for Simulated Hypo- and Hyper-attenuating Hepatic Tumors on MDCT. Academic Radiology, 2011, 18, 626-633.	2.5	3
340	Added value of 80kVp images to averaged 120kVp images in the detection of hepatocellular carcinomas in liver transplantation candidates using dual-source dual-energy MDCT: Results of JAFROC analysis. European Journal of Radiology, 2011, 80, e76-e85.	2.6	18
341	Comparison of accuracy and time-efficiency of CT colonography between conventional and panoramic 3D interpretation methods: An anthropomorphic phantom study. European Journal of Radiology, 2011, 80, e68-e75.	2.6	5
342	Liver metastases on quantitative color mapping of the arterial enhancement fraction from multiphasic CT scans: Evaluation of the hemodynamic features and correlation with the chemotherapy response. European Journal of Radiology, 2011, 80, e278-e283.	2.6	17

#	Article	IF	CITATIONS
343	Consensus Report of the 4th International Forum for Gadolinium-Ethoxybenzyl-Diethylenetriamine Pentaacetic Acid Magnetic Resonance Imaging. Korean Journal of Radiology, 2011, 12, 403.	3.4	57
344	Radiofrequency Ablation for Treating Liver Metastases from a Non-Colorectal Origin. Korean Journal of Radiology, 2011, 12, 579.	3.4	14
345	Dual-Energy Computed Tomography to Assess Tumor Response to Hepatic Radiofrequency Ablation. Investigative Radiology, 2011, 46, 77-84.	6.2	82
346	Negative hepatitis B envelope antigen predicts intrahepatic recurrence in hepatitis B virusâ€related hepatocellular carcinoma after ablation therapy. Journal of Gastroenterology and Hepatology (Australia), 2011, 26, 1638-1645.	2.8	17
347	Apparent diffusion coefficient for evaluating tumour response to neoadjuvant chemoradiation therapy for locally advanced rectal cancer. European Radiology, 2011, 21, 987-995.	4.5	162
348	Assessment of the treatment response of HCC. Abdominal Imaging, 2011, 36, 300-314.	2.0	52
349	Hepatocellular nodules in liver cirrhosis: MR evaluation. Abdominal Imaging, 2011, 36, 282-289.	2.0	53
350	Stress (Tako-Tsubo) Cardiomyopathy Following Radiofrequency Ablation of a Liver Tumor: A Case Report. CardioVascular and Interventional Radiology, 2011, 34, 86-89.	2.0	9
351	Imaging diagnosis and staging of hepatocellular carcinoma. Liver Transplantation, 2011, 17, S34-S43.	2.4	42
352	Gadoxetic acid disodiumâ€enhanced magnetic resonance imaging for biliary and vascular evaluations in preoperative living liver donors: Comparison with gadobenate dimeglumineâ€enhanced MRI. Journal of Magnetic Resonance Imaging, 2011, 33, 149-159.	3.4	46
353	MR elastography for noninvasive assessment of hepatic fibrosis: Experience from a tertiary center in asia. Journal of Magnetic Resonance Imaging, 2011, 34, 1110-1116.	3.4	86
354	CT Color Mapping of the Arterial Enhancement Fraction of VX2 Carcinoma Implanted in Rabbit Liver: Comparison With Perfusion CT. American Journal of Roentgenology, 2011, 196, 102-108.	2.2	26
355	Safety Margin Assessment After Radiofrequency Ablation of the Liver Using Registration of Preprocedure and Postprocedure CT Images. American Journal of Roentgenology, 2011, 196, W565-W572.	2.2	85
356	Gadoxetate Disodium–Enhanced Hepatobiliary Phase MRI of Hepatocellular Carcinoma: Correlation With Histological Characteristics. American Journal of Roentgenology, 2011, 197, 399-405.	2.2	54
357	Intrahepatic Mass-forming Cholangiocarcinomas: Enhancement Patterns at Multiphasic CT, with Special Emphasis on Arterial Enhancement Pattern—Correlation with Clinicopathologic Findings. Radiology, 2011, 260, 148-157.	7.3	200
358	Quantitative Color Mapping of the Arterial Enhancement Fraction in Patients With Diffuse Liver Disease. American Journal of Roentgenology, 2011, 197, 876-883.	2.2	42
359	Small (â‰ 2 0 mm) Pancreatic Adenocarcinomas: Analysis of Enhancement Patterns and Secondary Signs with Multiphasic Multidetector CT. Radiology, 2011, 259, 442-452.	7.3	212

Preoperative Imaging of Liver Cancers: Hepatocellular Carcinoma. , 2011, , 51-59.

0

Jeong Min Lee

#	Article	IF	CITATIONS
361	Image Fusion in Dual Energy Computed Tomography for Detection of Hypervascular Liver Hepatocellular Carcinoma. Investigative Radiology, 2010, 45, 149-157.	6.2	73
362	Gadoxetic Acid-Enhanced Magnetic Resonance Imaging for Differentiating Small Hepatocellular Carcinomas (â‰2 cm in Diameter) From Arterial Enhancing Pseudolesions. Investigative Radiology, 2010, 45, 96-103.	6.2	199
363	Consensus Report of the Third International Forum for Liver Magnetic Resonance Imaging. Investigative Radiology, 2010, 45, S1-S10.	6.2	4
364	Gadobutrol-enhanced, Three-Dimensional, Dynamic MR Imaging With MR Cholangiography for the Preoperative Evaluation of Bile Duct Cancer. Investigative Radiology, 2010, 45, 217-224.	6.2	39
365	Comparison of polyp distance on CT colonography between supine and prone scans using an automated path-distance measurement tool: correlation with colonoscopy. Abdominal Imaging, 2010, 35, 41-48.	2.0	Ο
366	Advancement in HCC imaging: diagnosis, staging and treatment efficacy assessments. Journal of Hepato-Biliary-Pancreatic Sciences, 2010, 17, 369-373.	2.6	53
367	Asian Pacific Association for the Study of the Liver consensus recommendations on hepatocellular carcinoma. Hepatology International, 2010, 4, 439-474.	4.2	944
368	Acoustic Radiation Force Impulse Elastography for Chronic Liver Disease: Comparison with Ultrasound-Based Scores of Experienced Radiologists, Child-Pugh Scores and Liver Function Tests. Ultrasound in Medicine and Biology, 2010, 36, 1637-1643.	1.5	54
369	Clinical Application of Liver MR Imaging in Wilson's Disease. Korean Journal of Radiology, 2010, 11, 665.	3.4	26
370	Differentiation of Intraductal Growing–type Cholangiocarcinomas from Nodular-type Cholangiocarcinomas at Biliary MR Imaging with MR Cholangiography. Radiology, 2010, 257, 364-372.	7.3	41
371	MR Imaging Features of Small Solid Pseudopapillary Tumors: Retrospective Differentiation From Other Small Solid Pancreatic Tumors. American Journal of Roentgenology, 2010, 195, 1324-1332.	2.2	76
372	Three-Dimensional MDCT for Preoperative Local Staging of Gastric Cancer Using Gas and Water Distention Methods: A Retrospective Cohort Study. American Journal of Roentgenology, 2010, 195, 1316-1323.	2.2	25
373	Small (â‰ 8 cm) Solid Pseudopapillary Tumors of the Pancreas at Multiphasic Multidetector CT. Radiology, 2010, 257, 97-106.	7.3	106
374	Diagnostic Performance of 64-Channel Multidetector CT in the Evaluation of Gastric Cancer: Differentiation of Mucosal Cancer (T1a) from Submucosal Involvement (T1b and T2). Radiology, 2010, 255, 805-814.	7.3	67
375	Computer-aided polyp detection on CT colonography: Comparison of three systems in a high-risk human population. European Journal of Radiology, 2010, 75, e147-e157.	2.6	8
376	MRI of magnetically labeled mesenchymal stem cells in hepatic failure model. World Journal of Gastroenterology, 2010, 16, 5611.	3.3	8
377	Primary Biliary Lymphoma Mimicking Cholangiocarcinoma: A Characteristic Feature of Discrepant CT and Direct Cholangiography Findings. Journal of Korean Medical Science, 2009, 24, 956.	2.5	21
378	Locally Advanced Rectal Cancer: Added Value of Diffusion-weighted MR Imaging in the Evaluation of Tumor Response to Neoadjuvant Chemo- and Radiation Therapy. Radiology, 2009, 253, 116-125.	7.3	325

#	Article	IF	CITATIONS
379	MRI Features of Pancreatic Colloid Carcinoma. American Journal of Roentgenology, 2009, 193, W308-W313.	2.2	31
380	Using Adobe Acrobat to Create High-Resolution Line Art Images. American Journal of Roentgenology, 2009, 193, W112-W117.	2.2	2
381	Ectopic Pancreas: CT Findings with Emphasis on Differentiation from Small Gastrointestinal Stromal Tumor and Leiomyoma. Radiology, 2009, 252, 92-100.	7.3	131
382	Quantitative CT Color Mapping of the Arterial Enhancement Fraction of the Liver to Detect Hepatocellular Carcinoma. Radiology, 2009, 250, 425-4s34.	7.3	70
383	Radiologist Performance in Differentiating Polypoid Early From Advanced Gastric Cancer Using Specific CT Criteria: Emphasis on Dimpling Sign. American Journal of Roentgenology, 2009, 193, 1546-1555.	2.2	3
384	Differential CT Features of Intraductal Biliary Metastasis and Double Primary Intraductal Polypoid Cholangiocarcinoma in Patients With a History of Extrabiliary Malignancy. American Journal of Roentgenology, 2009, 193, 1061-1069.	2.2	32
385	Multiphasic MDCT Enhancement Pattern of Hepatocellular Carcinoma Smaller Than 3 cm in Diameter: Tumor Size and Cellular Differentiation. American Journal of Roentgenology, 2009, 193, W482-W489.	2.2	113
386	Detection and characterization of focal hepatic lesions by T2-weighted imaging: comparison of navigator-triggered turbo spin-echo, breath-hold turbo spin-echo, and HASTE sequences. Clinical Imaging, 2009, 33, 281-288.	1.5	3
387	Differentiation of wellâ€differentiated hepatocellular carcinomas from other hepatocellular nodules in cirrhotic liver: Value of SPIOâ€enhanced MR imaging at 3.0 Tesla. Journal of Magnetic Resonance Imaging, 2009, 29, 328-335.	3.4	24
388	Accuracy of MRI for predicting the circumferential resection margin, mesorectal fascia invasion, and tumor response to neoadjuvant chemoradiotherapy for locally advanced rectal cancer. Journal of Magnetic Resonance Imaging, 2009, 29, 1093-1101.	3.4	61
389	Preoperative evaluation of pancreatic cancer: Comparison of gadoliniumâ€enhanced dynamic MRI with MR cholangiopancreatography versus MDCT. Journal of Magnetic Resonance Imaging, 2009, 30, 586-595.	3.4	136
390	Adenosquamous carcinoma of the extrahepatic bile duct: clinicopathologic and radiologic features. Abdominal Imaging, 2009, 34, 217-224.	2.0	10
391	Computer-aided image analysis of focal hepatic lesions in ultrasonography: preliminary results. Abdominal Imaging, 2009, 34, 183-191.	2.0	22
392	Usefulness of CT volumetry for primary gastric lesions in predicting pathologic response to neoadjuvant chemotherapy in advanced gastric cancer. Abdominal Imaging, 2009, 34, 430-440.	2.0	53
393	Magnetic resonance pancreatography: comparison of two- and three-dimensional sequences for assessment of intraductal papillary mucinous neoplasm of the pancreas. European Radiology, 2009, 19, 2163-2170.	4.5	14
394	Consensus report of the 2nd International Forum for Liver MRI. European Radiology, 2009, 19, 975-989.	4.5	125
395	Helical CT Evaluation of the Preoperative Staging of Gastric Cancer in the Remnant Stomach. American Journal of Roentgenology, 2009, 192, 902-908.	2.2	21
396	Multidetector Row Computed Tomographic Gastrography Findings After Endoscopic Submucosal Dissection for Early Gastric Cancer. Journal of Computer Assisted Tomography, 2009, 33, 273-279.	0.9	5

#	Article	IF	CITATIONS
397	Comparison Study of Different Bowel Preparation Regimens and Different Fecal-Tagging Agents on Tagging Efficacy, Patients' Compliance, and Diagnostic Performance of Computed Tomographic Colonography. Journal of Computer Assisted Tomography, 2009, 33, 657-665.	0.9	9
398	Differentiating Focal Eosinophilic Necrosis of the Liver From Hepatic Metastases Using Unenhanced and Portal Venous Phase Computed Tomographic Imagings. Journal of Computer Assisted Tomography, 2009, 33, 705-709.	0.9	8
399	Additional Value of SPIO-Enhanced MR Imaging for the Noninvasive Imaging Diagnosis of Hepatocellular Carcinoma in Cirrhotic Liver. Investigative Radiology, 2009, 44, 800-807.	6.2	20
400	Diagnostic Performance of Multidetector Row Computed Tomography, Superparamagnetic Iron Oxide-Enhanced Magnetic Resonance Imaging, and Dual-Contrast Magnetic Resonance Imaging in Predicting the Appropriateness of a Transplant Recipient Based on Milan Criteria. Investigative Radiology, 2009, 44, 311-321.	6.2	37
401	Evaluation of the Gross Type and Longitudinal Extent of Extrahepatic Cholangiocarcinomas on Contrast-Enhanced Multidetector Row Computed Tomography. Journal of Computer Assisted Tomography, 2009, 33, 376-382.	0.9	38
402	Gastrointestinal stromal tumor of the stomach: preliminary results of preoperative evaluation with CT gastrography. Abdominal Imaging, 2008, 33, 255-261.	2.0	23
403	Selection of Appropriate Liver Resection in Left Hepatolithiasis Based on Anatomic and Clinical Study. World Journal of Surgery, 2008, 32, 413-418.	1.6	28
404	Navigatorâ€ŧriggered isotropic threeâ€dimensional magnetic resonance cholangiopancreatography in the diagnosis of malignant biliary obstructions: Comparison with direct cholangiography. Journal of Magnetic Resonance Imaging, 2008, 27, 94-101.	3.4	39
405	MR imaging findings of early bile duct cancer. Journal of Magnetic Resonance Imaging, 2008, 28, 1466-1475.	3.4	20
406	Treatment Guidelines for Branch Duct Type Intraductal Papillary Mucinous Neoplasms of the Pancreas: When Can We Operate or Observe?. Annals of Surgical Oncology, 2008, 15, 199-205.	1.5	165
407	Intrahepatic Extramedullary Hematopoiesis Mimicking a Hypervascular Hepatic Neoplasm on Dynamic- and SPIO-Enhanced MRI. Korean Journal of Radiology, 2008, 9, S34.	3.4	19
408	Magnetic resonance cholangiography: comparison of two- and three-dimensional sequences for assessment of malignant biliary obstruction. European Radiology, 2008, 18, 78-86.	4.5	24
409	Optimal interventional treatment and longâ€ŧerm outcomes for biliary stricture after liver transplantation. Clinical Transplantation, 2008, 22, 484-493.	1.6	41
410	Enhancement characteristics of cholangiocarcinomas on mutiphasic helical CT: emphasis on morphologic subtypes. Clinical Imaging, 2008, 32, 114-120.	1.5	30
411	Detection and characterization of focal hepatic lesions: comparative study of MDCT and gadobenate dimeglumine-enhanced MR imaging. Clinical Imaging, 2008, 32, 287-295.	1.5	12
412	Diffusion-Weighted MR. Academic Radiology, 2008, 15, 593-600.	2.5	27
413	Diagnostic Accuracy of Multi-/Single-Detector Row CT and Contrast-Enhanced MRI in the Detection of Hepatocellular Carcinomas Meeting the Milan Criteria before Liver Transplantation. Intervirology, 2008, 51, 52-60.	2.8	48
414	Analysis of Enhancement Pattern of Flat Gallbladder Wall Thickening on MDCT to Differentiate Gallbladder Cancer from Cholecystitis. American Journal of Roentgenology, 2008, 191, 765-771.	2.2	98

#	Article	IF	CITATIONS
415	Hilar Cholangiocarcinoma: Role of Preoperative Imaging with Sonography, MDCT, MRI, and Direct Cholangiography. American Journal of Roentgenology, 2008, 191, 1448-1457.	2.2	103
416	Changes of Portosystemic Collaterals and Splenic Volume on CT After Liver Transplantation and Factors Influencing Those Changes. American Journal of Roentgenology, 2008, 191, W8-W16.	2.2	42
417	Sonography Transmission Gel as Endorectal Contrast Agent for Tumor Visualization in Rectal Cancer. American Journal of Roentgenology, 2008, 191, 186-189.	2.2	33
418	Accuracy of Preoperative T-Staging of Gallbladder Carcinoma Using MDCT. American Journal of Roentgenology, 2008, 190, 74-80.	2.2	106
419	Hepatocellular Carcinoma in Liver Transplantation Candidates: Detection with Gadobenate Dimeglumine–Enhanced MRI. American Journal of Roentgenology, 2008, 191, 529-536.	2.2	82
420	Effects of Spatial Resolution and Tube Current on Computer-aided Detection of Polyps on CT Colonographic Images: Phantom Study. Radiology, 2008, 248, 492-503.	7.3	22
421	Preoperative Evaluation of Bile Duct Cancer: MRI Combined with MR Cholangiopancreatography Versus MDCT with Direct Cholangiography. American Journal of Roentgenology, 2008, 190, 396-405.	2.2	148
422	High-Definition Flow Doppler Ultrasonographic Technique to Assess Hepatic Vasculature Compared With Color or Power Doppler Ultrasonography. Journal of Ultrasound in Medicine, 2008, 27, 1491-1501.	1.7	28
423	Biliary Malignancy. Journal of Computer Assisted Tomography, 2008, 32, 362-368.	0.9	19
424	Diagnostic Accuracy of 3.0-Tesla Rectal Magnetic Resonance Imaging in Preoperative Local Staging of Primary Rectal Cancer. Investigative Radiology, 2008, 43, 587-593.	6.2	38
425	Hepatocellular Carcinoma in Cirrhotic Liver: Double-Contrast-Enhanced, High-Resolution 3.0T-MR Imaging With Pathologic Correlation. Investigative Radiology, 2008, 43, 538-546.	6.2	35
426	The Value of Gadobenate Dimeglumine-Enhanced Delayed Phase MR Imaging for Characterization of Hepatocellular Nodules in the Cirrhotic Liver. Investigative Radiology, 2008, 43, 202-210.	6.2	67
427	Intrapancreatic Accessory Spleen: Findings on MR Imaging, CT, US and Scintigraphy, and the Pathologic Analysis. Korean Journal of Radiology, 2008, 9, 162.	3.4	107
428	The Association of Anisakiasis in the Ascending Colon with Sigmoid Colon Cancer: CT Colonography Findings. Korean Journal of Radiology, 2008, 9, S56.	3.4	15
429	Peripheral Mass–Forming Cholangiocarcinoma in Cirrhotic Liver. American Journal of Roentgenology, 2007, 189, 1428-1434.	2.2	114
430	Computer-Aided Detection of Colonic Polyps at CT Colonography Using a Hessian Matrix–Based Algorithm: Preliminary Study. American Journal of Roentgenology, 2007, 189, 41-51.	2.2	30
431	Detection of Hepatocellular Carcinoma on CT in Liver Transplant Candidates: Comparison of PACS Tile and Multisynchronized Stack Modes. American Journal of Roentgenology, 2007, 188, 1337-1342.	2.2	10
432	Two- versus Three-dimensional Colon Evaluation with Recently Developed Virtual Dissection Software for CT Colonography. Radiology, 2007, 244, 852-864.	7.3	51

#	Article	IF	CITATIONS
433	Contrast-Enhanced Sonography of Intrapancreatic Accessory Spleen in Six Patients. American Journal of Roentgenology, 2007, 188, 422-428.	2.2	42
434	Esophageal Varices in Patients with Cirrhosis: Multidetector CT Esophagography—Comparison with Endoscopy. Radiology, 2007, 242, 759-768.	7.3	98
435	Three-dimensional MDCT Gastrography Compared With Axial CT for the Detection of Early Gastric Cancer. Journal of Computer Assisted Tomography, 2007, 31, 741-749.	0.9	17
436	Hepatic Venous Congestion After Right-lobe Living-donor Liver Transplantation. Journal of Computer Assisted Tomography, 2007, 31, 181-187.	0.9	14
437	Multiple-Electrode Radiofrequency Ablation of In Vivo Porcine Liver. Investigative Radiology, 2007, 42, 676-683.	6.2	46
438	Differentiating Malignant From Benign Wall Thickening in Postoperative Stomach Using Helical Computed Tomography. Journal of Computer Assisted Tomography, 2007, 31, 455-462.	0.9	5
439	Switching Monopolar Radiofrequency Ablation Technique Using Multiple, Internally Cooled Electrodes and a Multichannel Generator. Investigative Radiology, 2007, 42, 163-171.	6.2	55
440	Recurrence Patterns of Combined Hepatocellular-Cholangiocarcinoma on Enhanced Computed Tomography. Journal of Computer Assisted Tomography, 2007, 31, 109-115.	0.9	25
441	Evaluation of the Longitudinal Tumor Extent of Bile Duct Cancer. Journal of Computer Assisted Tomography, 2007, 31, 469-474.	0.9	17
442	Focal Peliosis Hepatis as a Mimicker of Hepatic Tumors. Journal of Computer Assisted Tomography, 2007, 31, 79-85.	0.9	54
443	In Vivo Efficiency of Multipolar Radiofrequency Ablation with Two Bipolar Electrodes: A Comparative Experimental Study in Pig Kidney. Journal of Vascular and Interventional Radiology, 2007, 18, 1553-1560.	0.5	12
444	A New and Simple Practical Plane Dividing Hepatic Segment 2 and 3 of the Liver: Evaluation of Its Validity. Korean Journal of Radiology, 2007, 8, 302.	3.4	9
445	Routine intraoperative Doppler sonography in the evaluation of complications after living-related donor liver transplantation. Journal of Clinical Ultrasound, 2007, 35, 483-490.	0.8	22
446	Classification and prognosis of intrahepatic biliary stricture after liver transplantation. Liver Transplantation, 2007, 13, 1736-1742.	2.4	91
447	Contrastâ€enhanced MRI combined with MR cholangiopancreatography for the evaluation of patients with biliary strictures: Differentiation of malignant from benign bile duct strictures. Journal of Magnetic Resonance Imaging, 2007, 26, 304-312.	3.4	75
448	Differentiation of intraductal papillary mucinous neoplasms from other pancreatic cystic masses: Comparison of multirowâ€detector CT and MR imaging using ROC analysis. Journal of Magnetic Resonance Imaging, 2007, 26, 86-93.	3.4	132
449	Preoperative evaluation of hepatic arterial and portal venous anatomy using the time resolved echo-shared MR angiographic technique in living liver donors. European Radiology, 2007, 17, 1074-1080.	4.5	24
450	Assessment of hilar and extrahepatic bile duct cancer using multidetector CT: value of adding multiplanar reformations to standard axial images. European Radiology, 2007, 17, 3130-3138.	4.5	25

#	Article	IF	CITATIONS
451	Gastric hepatoid adenocarcinoma: CT findings. Abdominal Imaging, 2007, 32, 293-298.	2.0	21
452	Radiofrequency Ablation of the Porcine Liver In Vivo: Increased Coagulation with an Internally Cooled Perfusion Electrode. Academic Radiology, 2006, 13, 343-352.	2.5	30
453	Comparison of fundamental sonography, tissue-harmonic sonography, fundamental compound sonography, and tissue-harmonic compound sonography for focal hepatic lesions. European Radiology, 2006, 16, 2444-2453.	4.5	21
454	Radiofrequency Renal Ablation: In Vivo Comparison of Internally Cooled, Multitined Expandable and Internally Cooled Perfusion Electrodes. Journal of Vascular and Interventional Radiology, 2006, 17, 549-556.	0.5	8
455	Preoperative Assessment of Resectability of Hepatic Hilar Cholangiocarcinoma: Combined CT and Cholangiography with Revised Criteria. Radiology, 2006, 239, 113-121.	7.3	200
456	State-of-the-art ultrasonography of hepatocellular carcinoma. European Journal of Radiology, 2006, 58, 177-185.	2.6	7
457	Efficacy and safety of radiofrequency ablation of hepatocellular carcinoma in the hepatic dome with the CT-guided extrathoracic transhepatic approach. European Journal of Radiology, 2006, 60, 100-107.	2.6	28
458	Intraoperative Radiofrequency Ablation Using a Loop Internally Cooled-Perfusion Electrode: In Vitro and In Vivo Experiments. Journal of Surgical Research, 2006, 131, 215-224.	1.6	4
459	Hepatic Radiofrequency Ablation Using Multiple Probes: Ex Vivo and In Vivo Comparative Studies of Monopolar versus Multipolar Modes. Korean Journal of Radiology, 2006, 7, 106.	3.4	26
460	Superparamagnetic Iron Oxide-Enhanced Liver Magnetic Resonance Imaging. Investigative Radiology, 2006, 41, 168-174.	6.2	43
461	Computed Tomography Features of an Intraductal Polypoid Mass. Journal of Computer Assisted Tomography, 2006, 30, 18-24.	0.9	6
462	CT Features of an Intraductal Polypoid Mass. Journal of Computer Assisted Tomography, 2006, 30, 173-181.	0.9	35
463	High-grade Neuroendocrine Carcinomas of the Gallbladder and Bile Duct. Journal of Computer Assisted Tomography, 2006, 30, 604-609.	0.9	54
464	Solid Organizing Hepatic Abscesses Mimic Hepatic Tumor. Journal of Computer Assisted Tomography, 2006, 30, 189-196.	0.9	15
465	MDCT and superparamagnetic iron oxide (SPIO)-enhanced MR findings of intrapancreatic accessory spleen in seven patients. European Radiology, 2006, 16, 1887-1897.	4.5	62
466	The diagnostic value of multiplanar reconstruction on MDCT colonography for the preoperative staging of colorectal cancer. European Radiology, 2006, 16, 2284-2291.	4.5	28
467	Three-dimensional MDCT imaging and CT esophagography for evaluation of esophageal tumors: preliminary study. European Radiology, 2006, 16, 2418-2426.	4.5	24
468	Preoperative evaluation of the hepatic vascular anatomy in living liver donors: Comparison of CT angiography and MR angiography. Journal of Magnetic Resonance Imaging, 2006, 24, 1081-1087.	3.4	45

#	Article	IF	CITATIONS
469	Comparison of Gadobenate Dimeglumine-Enhanced Dynamic MRI and 16-MDCT for the Detection of Hepatocellular Carcinoma. American Journal of Roentgenology, 2006, 186, 149-157.	2.2	92
470	Radiofrequency Ablation of Hepatocellular Carcinoma in Patients with Decompensated Cirrhosis: Evaluation of Therapeutic Efficacy and Safety. American Journal of Roentgenology, 2006, 186, S261-S268.	2.2	19
471	Macrocystic Neoplasms of the Pancreas: CT Differentiation of Serous Oligocystic Adenoma from Mucinous Cystadenoma and Intraductal Papillary Mucinous Tumor. American Journal of Roentgenology, 2006, 187, 1192-1198.	2.2	146
472	Gadobenate Dimeglumine-Enhanced Liver MRI as the Sole Preoperative Imaging Technique: A Prospective Study of Living Liver Donors. American Journal of Roentgenology, 2006, 187, 1223-1233.	2.2	50
473	Hepatic Macrosteatosis: Predicting Appropriateness of Liver Donation by Using MR Imaging—Correlation with Histopathologic Findings. Radiology, 2006, 240, 116-129.	7.3	71
474	Percutaneous Drainage of Postoperative Abdominal Abscess with Limited Accessibility: Preexisting Surgical Drains as Alternative Access Route. Radiology, 2006, 239, 591-598.	7.3	26
475	CT Differentiation of Cholangiocarcinoma from Periductal Fibrosis in Patients with Hepatolithiasis. American Journal of Roentgenology, 2006, 187, 445-453.	2.2	43
476	Hepatocellular Carcinoma in Patients with Chronic Liver Disease: Comparison of SPIO-enhanced MR Imaging and 16–Detector Row CT. Radiology, 2006, 238, 531-541.	7.3	109
477	Bipolar radiofrequency ablation in ex vivo bovine liver with the open-perfused system versus the cooled-wet system. European Radiology, 2005, 15, 759-764.	4.5	27
478	Detection of hepatocellular carcinoma: comparison of ferumoxides-enhanced and gadolinium-enhanced dynamic three-dimensional volume interpolated breath-hold MR imaging. European Radiology, 2005, 15, 140-147.	4.5	22
479	Detection of liver metastases: gadobenate dimeglumine-enhanced three-dimensional dynamic phases and one-hour delayed phase MR imaging versus superparamagnetic iron oxide-enhanced MR imaging. European Radiology, 2005, 15, 220-228.	4.5	84
480	Radiofrequency ablation in the liver using two cooled-wet electrodes in the bipolar mode. European Radiology, 2005, 15, 2163-2170.	4.5	16
481	Ex Vivo Experiment of Saline-Enhanced Hepatic Bipolar Radiofrequency Ablation with a Perfused Needle Electrode: Comparison with Conventional Monopolar and Simultaneous Monopolar Modes. CardioVascular and Interventional Radiology, 2005, 28, 338-345.	2.0	30
482	Biliary Complications in Living Donor Liver Transplantation: Imaging Findings and the Roles of Interventional Procedures. CardioVascular and Interventional Radiology, 2005, 28, 756-767.	2.0	35
483	Radiofrequency Thermal Ablation in Canine Femur: Evaluation of Coagulation Necrosis Reproducibility and MRI-Histopathologic Correlation. American Journal of Roentgenology, 2005, 185, 661-667.	2.2	27
484	Appropriateness of a Donor Liver with Respect to Macrosteatosis: Application of Artificial Neural Networks to US Images—Initial Experience. Radiology, 2005, 234, 793-803.	7.3	70
485	Differentiating Malignant from Benign Common Bile Duct Stricture with Multiphasic Helical CT. Radiology, 2005, 236, 178-183.	7.3	107
486	Value of Contrast-Enhanced Sonography for the Characterization of Focal Hepatic Lesions in Patients with Diffuse Liver Disease: Receiver Operating Characteristic Analysis. American Journal of Roentgenology, 2005, 184, 1077-1084.	2.2	53

#	Article	IF	CITATIONS
487	Postbiopsy Splenic Bleeding in a Dog Model: Comparison of Cauterization, Embolization, and Plugging of the Needle Tract. American Journal of Roentgenology, 2005, 185, 878-884.	2.2	23
488	Comparison of Renal Ablation with Monopolar Radiofrequency and Hypertonic-Saline-Augmented Bipolar Radiofrequency: In Vitro and In Vivo Experimental Studies. American Journal of Roentgenology, 2005, 184, 897-905.	2.2	28
489	Feasibility of Application of Sensitivity Encoding to the Breath-Hold T2-Weighted Turbo Spin-Echo Sequence for Evaluation of Focal Hepatic Tumors. American Journal of Roentgenology, 2005, 184, 497-504.	2.2	8
490	Effect of Adjusted Positioning on Gastric Distention and Fluid Distribution During CT Gastrography. American Journal of Roentgenology, 2005, 185, 1180-1184.	2.2	33
491	MRI Findings of Focal Eosinophilic Liver Diseases. American Journal of Roentgenology, 2005, 184, 1541-1548.	2.2	40
492	Small-Bowel Obstruction in a Phantom Model of ex Vivo Porcine Intestine: Comparison of PACS Stack and Tile Modes for CT Interpretation. Radiology, 2005, 236, 867-871.	7.3	13
493	Bipolar Radiofrequency Ablation Using Wet-Cooled Electrodes: An In Vitro Experimental Study in Bovine Liver. American Journal of Roentgenology, 2005, 184, 391-397.	2.2	31
494	An ex-vivo experimental study on optimization of bipolar radiofrequency liver ablation using perfusion-cooled electrodes. Acta Radiologica, 2005, 46, 443-451.	1.1	16
495	In vitro CT evaluation of intrahepatic stones: correlation with chemical composition. European Journal of Radiology, 2005, 54, 258-263.	2.6	2
496	Wet radio-frequency ablation using multiple electrodes: comparative study of bipolar versus monopolar modes in the bovine liver. European Journal of Radiology, 2005, 54, 408-417.	2.6	21
497	Optimization of Wet Radiofrequency Ablation Using a Perfused-Cooled Electrode: A Comparative Study in Ex Vivo Bovine Livers. Korean Journal of Radiology, 2004, 5, 250.	3.4	14
498	Combined Radiofrequency Ablation and Acetic Acid Hypertonic Saline Solution Instillation: An In Vivo Study of Rabbit Liver. Korean Journal of Radiology, 2004, 5, 31.	3.4	5
499	Cystic Changes in Intraabdominal Extrahepatic Metastases from Gastrointestinal Stromal Tumors Treated with Imatinib. Korean Journal of Radiology, 2004, 5, 157.	3.4	6
500	Saline-Enhanced Hepatic Radiofrequency Ablation Using a Perfused-Cooled Electrode: Comparison of Dual Probe Bipolar Mode with Monopolar and Single Probe Bipolar Modes. Korean Journal of Radiology, 2004, 5, 121.	3.4	25
501	Comparison of Wet Radiofrequency Ablation with Dry Radiofrequency Ablation and Radiofrequency Ablation Using Hypertonic Saline Preinjection: Ex Vivo Bovine Liver. Korean Journal of Radiology, 2004, 5, 258.	3.4	34
502	MRI for Detection of Hepatocellular Carcinoma: Comparison of Mangafodipir Trisodium and Gadopentetate Dimeglumine Contrast Agents. American Journal of Roentgenology, 2004, 183, 1049-1054.	2.2	32
503	Comparison of Superparamagnetic Iron Oxide–Enhanced and Gadobenate Dimeglumine–Enhanced Dynamic MRI for Detection of Small Hepatocellular Carcinomas. American Journal of Roentgenology, 2004, 182, 1217-1223.	2.2	43
504	Primary and Secondary Lung Malignancies Treated with Percutaneous Radiofrequency Ablation: Evaluation with Follow-Up Helical CT. American Journal of Roentgenology, 2004, 183, 1013-1020.	2.2	78

#	Article	IF	CITATIONS
505	Percutaneous Radiofrequency Ablation for Inoperable Non–Small Cell Lung Cancer and Metastases: Preliminary Report. Radiology, 2004, 230, 125-134.	7.3	332
506	Acute Cerebral Infarction After Radiofrequency Ablation of an Atypical Carcinoid Pulmonary Tumor. American Journal of Roentgenology, 2004, 182, 990-992.	2.2	37
507	Gastrointestinal Stromal Tumors of the Stomach: CT Findings and Prediction of Malignancy. American Journal of Roentgenology, 2004, 183, 893-898.	2.2	93
508	Relationship Between Various Patterns of Transient Increased Hepatic Attenuation on CT and Portal Vein Thrombosis Related to Acute Cholecystitis. American Journal of Roentgenology, 2004, 183, 437-442.	2.2	28
509	Volumetric Contrast Imaging in Bile Duct Sonography:Technology and Early Clinical Experience. American Journal of Roentgenology, 2004, 183, 1602-1604.	2.2	2
510	Intussusception in Adults: From Stomach to Rectum. American Journal of Roentgenology, 2004, 183, 691-698.	2.2	92
511	Gadobenate dimeglumine-enhanced liver MR imaging: value of dynamic and delayed imaging for the characterization and detection of focal liver lesions. European Radiology, 2004, 14, 5-13.	4.5	102
512	Combined treatment of radiofrequency ablation and acetic acid injection: an in vivo feasibility study in rabbit liver. European Radiology, 2004, 14, 1303-10.	4.5	20
513	Four-dimensional volume contrast ultrasound imaging of the gallbladder compared with tissue harmonic imaging: preliminary experience. European Radiology, 2004, 14, 1657-64.	4.5	6
514	Combined Therapy of Radiofrequency Ablation and Ethanol Injection of Rabbit Liver: An In Vivo Feasibility Study. CardioVascular and Interventional Radiology, 2004, 27, 151-7.	2.0	9
515	Threeâ€dimensional dynamic liver MR imaging using sensitivity encoding for detection of hepatocellular carcinomas: Comparison with superparamagnetic iron oxideâ€enhanced MR imaging. Journal of Magnetic Resonance Imaging, 2004, 20, 826-837.	3.4	44
516	Primary Gastrointestinal Stromal Tumors in the Omentum and Mesentery: CT Findings and Pathologic Correlations. American Journal of Roentgenology, 2004, 182, 1463-1467.	2.2	48
517	Gastrointestinal Stromal Tumors of the Duodenum: CT and Barium Study Findings. American Journal of Roentgenology, 2004, 183, 415-419.	2.2	23
518	Imaging of Gastrointestinal Stromal Tumors. Journal of Computer Assisted Tomography, 2004, 28, 596-604.	0.9	35
519	Dual-Probe Radiofrequency Ablation. Investigative Radiology, 2004, 39, 89-96.	6.2	17
520	Sonographic Features of an Intraductal Polypoid Mass. Journal of Ultrasound in Medicine, 2004, 23, 1283-1291.	1.7	7
521	MR findings of renal malignant fibrous histiocytoma. European Radiology, 2003, 13, L245-L246.	4.5	5
522	Radio-frequency thermal ablation with hypertonic saline solution injection of the lung: ex vivo and in vivo feasibility studies. European Radiology, 2003, 13, 2540-2547.	4.5	76

#	Article	IF	CITATIONS
523	Open radio-frequency thermal ablation of renal VX2 tumors in a rabbit model using a cooled-tip electrode: feasibility, safety, and effectiveness. European Radiology, 2003, 13, 1324-1332.	4.5	33
524	Major Complications after Radio-frequency Thermal Ablation of Hepatic Tumors: Spectrum of Imaging Findings. Radiographics, 2003, 23, 123-134.	3.3	320
525	Percutaneous Radiofrequency Thermal Ablation of Lung VX2 Tumors in a Rabbit Model Using a Cooled Tip-Electrode. Investigative Radiology, 2003, 38, 129-139.	6.2	36
526	Combined Radiofrequency Ablation and Hot Saline Injection in Rabbit Liver. Investigative Radiology, 2003, 38, 725-732.	6.2	10
527	Contrastâ€Enhanced Agent Detection Imaging. Journal of Ultrasound in Medicine, 2003, 22, 897-910.	1.7	42
528	Therapeutic Response Evaluation of Malignant Hepatic Masses Treated by Interventional Procedures With Contrastâ€Enhanced Agent Detection Imaging. Journal of Ultrasound in Medicine, 2003, 22, 911-920.	1.7	30
529	Detection of Small Hypervascular Hepatocellular Carcinomas in Cirrhotic Patients: Comparison of Superparamagnetic Iron Oxide-Enhanced MR Imaging with Dual-Phase Spiral CT. Korean Journal of Radiology, 2003, 4, 1.	3.4	30
530	Characterization of Focal Liver Lesions with Superparamagnetic Iron Oxide-Enhanced MR Imaging: Value of Distributional Phase T1-Weighted Imaging. Korean Journal of Radiology, 2003, 4, 9.	3.4	12
531	A Comparative Experimental Study of the In-vitro Efficiency of Hypertonic Saline-Enhanced Hepatic Bipolar and Monopolar Radiofrequency Ablation. Korean Journal of Radiology, 2003, 4, 163.	3.4	56
532	Percutaneous Radiofrequency Thermal Ablation with Hypertonic Saline Injection: In Vivo Study in a Rabbit Liver Model. Korean Journal of Radiology, 2003, 4, 27.	3.4	35
533	Detection of Hepatic VX2 Tumors in Rabbits: Comparison of Conventional US and Phase-Inversion Harmonic US During the Liver-Specific Late Phase of Contrast Enhancement. Korean Journal of Radiology, 2003, 4, 124.	3.4	2
534	Hepatic Arterioportal Shunts: Dynamic CT and MR Features. Korean Journal of Radiology, 2002, 3, 1.	3.4	110
535	Saline-Enhanced Radiofrequency Thermal Ablation of the Lung: A Feasibility Study in Rabbits. Korean Journal of Radiology, 2002, 3, 245.	3.4	17
536	Mn-DPDP-enhanced MR Imaging: the Optimal Pulse Sequence for Detection of Focal Hepatic Tumor. Journal of the Korean Radiological Society, 2002, 46, 367.	0.0	0
537	Usefulness of Three-dimensional Contrast-Enhanced MR Angiography in the Evaluation of Pelvic and Lower Extremity Arteries. Journal of the Korean Radiological Society, 2002, 47, 573.	0.0	0
538	Contrast-Enhanced Three-Dimensional MR Imaging Using a Volumetric Interpolated Breath-hold Examination (VIBE): Clinical Utility in the Evaluation of Renal Tumors. Journal of the Korean Radiological Society, 2002, 47, 635.	0.0	0
539	Gadobenate Dimeglumine-enhanced MR of VX2 Carcinoma in Rabbit Liver: Usefulness of the Delayed Phase Imaging and Optimal Pulse Sequence. Journal of the Korean Radiological Society, 2002, 47, 51.	0.0	0
540	The Usefulness of T2-weighted MR Urography and Contrast Enhanced MR Urography in the Evaluation of Obstructive Uropathy: Comparisonal Study with Antegrade Pyelography1. Journal of the Korean Radiological Society, 2002, 46, 49.	0.0	0

#	Article	IF	CITATIONS
541	Ultrasound-Guided Radiofrequency Thermal Ablation of Normal Kidney in a Rabbit Model: Correlation with CT and Histopathology. Journal of the Korean Radiological Society, 2002, 46, 25.	0.0	1
542	Fluoroscopic-guided Covered Metallic Stent Placement for Gastric Outlet Obstruction and Post-operative Gastroenterostomy Anastomotic Stricture. Clinical Radiology, 2001, 56, 560-567.	1.1	26
543	MR Imaging-Histopathologic Correlation of Radiofrequency Thermal Ablation Lesion in a Rabbit Liver Model: Observation during Acute and Chronic Stages. Korean Journal of Radiology, 2001, 2, 151.	3.4	101
544	Ankle Ligaments: Comparison of MR Arthrography with Conventional MR Imaging in Amputated Feet. Journal of the Korean Radiological Society, 2001, 44, 513.	0.0	0
545	Radiofrequency Tissue Ablation with Cooled-Tip Electrodes:An Experimental Study in a Bovine Liver Model on Variables Influencing Lesion Size. Journal of the Korean Radiological Society, 2001, 44, 351.	0.0	1
546	Differentiation between Tuberculous and Pyogenic Spondylitis on Gd-enhanced MR Imaging: Focus on the Patterns of Disc Enhancement. Journal of the Korean Radiological Society, 2001, 45, 243.	0.0	0
547	Palliation of Malignant Gastric Obstruction: Fluoroscopic-Guided Covered Metallic Stent Placement. Journal of the Korean Radiological Society, 2000, 42, 459.	0.0	3
548	CT Findings of Ciliated Hepatic Foregut Cyst Mimicking Metastasis: A Case Report. Journal of the Korean Radiological Society, 2000, 43, 77.	0.0	2
549	Intraperitoneal Hemorrhage Due to Spontaneous Rupture of Hepatocellular Carcinoma: Comparisons of Tranarterial Oily Chemoembolization and Simple Embolization with Gelfoam. Journal of the Korean Radiological Society, 2000, 43, 171.	0.0	0
550	Hemangioma and Hepatocellular Carcinoma: Distinction with Superparamagnetic Iron Oxide-Enhanced MR Imaging. Journal of the Korean Radiological Society, 2000, 43, 195.	0.0	0
551	Superparamagnetic Iron Oxide Enhanced MR Imaging: Influence of Hepatic Dysfunction in Cirrhotic Patients. Journal of the Korean Radiological Society, 2000, 43, 319.	0.0	0
552	Excretory MR Urography Using Breathhold Three-dimensional FISP: Comparison with MR Urography Using HASTE Technique. Journal of the Korean Radiological Society, 2000, 43, 331.	0.0	0
553	CT findings of extramedullary hematopoiesis in the thorax, liver and kidneys, in a patient with idiopathic myelofibrosis. Journal of Korean Medical Science, 2000, 15, 460.	2.5	36
554	CT-guided celiac plexus block for intractable abdominal pain. Journal of Korean Medical Science, 2000, 15, 173.	2.5	48
555	Fluoroscopically Guided Biopsy of Intrathoracic Lesions: Diagnostic Accuracy of Combined Method Including Automated Gun Biopsy and Fine Needle Aspiration. Journal of the Korean Radiological Society, 2000, 43, 53.	0.0	0
556	SPIO-enhanced MR Imaging for HCC Detection in Cirrhotic Patient: Comparison of Various Techniques for Optimal Sequence Selection. Journal of the Korean Radiological Society, 2000, 42, 787.	0.0	0
557	Bronchial Arterial Embolization for Hemoptysis: Analysis of Outcome in Various Underlying Causes. Journal of the Korean Radiological Society, 1999, 41, 45.	0.0	3
558	CT and MR Findings of Primary Hepatic Leiomyosarcoma: A Case Report. Journal of the Korean Radiological Society, 1997, 37, 1087.	0.0	0

#	Article	IF	CITATIONS
559	Magnetic resonance cholangiopancreatography. , 0, , 123-133.		0
560	Clinical Utility of MicroPure US Imaging for Breast Microcalcifications. Journal of the Korean Society of Radiology, 0, 83, .	0.2	0
561	Analysis of clinical phenotypes of neuropathic symptoms in patients with type 2 diabetes: A multicenter study. Journal of Diabetes Investigation, 0, , .	2.4	Ο